NUMERICAL ANALYSIS OF FLEXURAL BEHAVIOUR OF CONCRETE FILLED STEEL TUBES(CFST) WITH TWO DIFFERENT CONCRETE INFILL

PROJECT REPORT

Submitted by

FEBIN FATHIMA N M

ROLL NO: M20CESC09

to

the A P J Abdul Kalam Technological University

in partial fulfillment of the requirements for the award of the Degree

of

Master of Technology

in

Structural Engineering & Construction Management

Department of Civil Engineering

T.K.M. College of Engineering, Kollam-691005

2022

DECLARATION

I undersigned hereby declare that the project report "Numerical Analysis of flexural behavior of concrete filled steel tubes (CFST) using two different concrete infills", submitted for partial fulfillment of the requirements for the award of degree of Master of Technology of the APJ Abdul Kalam Technological University, Kerala is a bonafide work done by me under supervision of Dr.Chinsu Mereena Joy, Assistant Professor, Department of Civil Engineering. This submission represents my ideas in my own words and where ideas or words of others have been included; I have adequately and accurately cited and referenced the original sources. I also declare that I have adhered to ethics of academic honesty and integrity and have not misrepresented or fabricated any data or idea or fact or source in my submission. I understand that any violation of the above will be a cause for disciplinary action by the institute and/or the University and can also evoke penal action from the sources which have thus not been properly cited or from whom proper permission has not been obtained. This report has not been previously formed the basis for the award of any degree, diploma or similar title of any other University.

KOLLAM FEBIN FATHIMA NM

DEPARTMENT OF CIVIL ENGINEERING
T.K.M. College of Engineering, Kollam

CERTIFICATE

Certified that this report entitled **'NUMERICAL ANALYSIS OF FLEXURAL BEHAVIOUR OF CONCRETE FILLED STEEL TUBES (CFST) USING TWO DIFFERENT CONCRETE INFILLS'** is the report of project presented by FEBIN FATHIMA N M , Roll No: M20CESC09 during 2021-2022 in partial fulfillment of the requirements for the award of the Degree of Master of Technology in Structural Engineering & Construction Management of the A. P. J. Abdul Kalam Technological University.

Guide	Coordinator	Head of the Department
Dr. Chinsu Mereena Joy	**Dr. Ramaswamy K. P.**	**Dr. Sajeeb R.**
Assistant Professor	Assistant Professor	Professor
Dept. of Civil Engineering	Dept. of Civil Engineering	Dept. of Civil Engineering

. ACKNOWLEDGEMENT

I take this opportunity to express my deep sense of gratitude and sincere thanks to all who helped me to complete the project successfully. I am deeply indebted to my guide, Dr. Chinsu Mereena Joy, Assistant Professor, Department of Civil Engineering for her excellent guidance, positive criticism and valuable comments.

I am greatly thankful to my project coordinator, Dr. Ramaswamy K.P., Assistant Professor, Department of Civil Engineering for their constant supervision as well as for providing necessary information regarding the project. I am greatly thankful to Dr. Sajeeb R., Professor and Head of the Department of Civil Engineering, for her kind support.

Finally, I thank my parents and friends who directly and indirectly contributed to the successful completion of my project. Above all, I thank the almighty God for the successful conduct of this project.

FEBIN FATHIMA N M

ABSTRACT

The main goal of this research is set out to study the flexural behaviour of concrete filled steel tubes (CFST) giving insight to two different concrete infills and their behaviour in different parametric combinations. A numerical study is done on high strength concrete filled CFST and geopolymer filled CFSTs. Separate models were used for both high strength concrete and geopolymer concrete.

The numerical investigation is done using ANSYS software. The Drucker Prager (DP) model is used for modelling the concrete. An extensive parametric study was performed to investigate the influences of depth-to-thickness ratio (28.57−200), effect of D/B ratio (24-42.8) and steel yield strengths (235–420 MPa) on the fundamental behavior of CFST beams under flexure load. When the D/B ratio increased from 0.54 to 2, the ultimate capacity of members is increased by more than 50%. In the analysis, the geopolymer filled CFST was able to take more load as compared with the high strength concrete. It can be seen that by increasing D/t ratio from 28.57 to 200 (7 times), the ultimate bending moment capacity reduced from 207.8 to 21 kNm (almost 8 times) for square CFST beams. The ultimate flexure strength of square CFST beams was found to increase significantly with an increase in the yield strength of steel. By increasing the yield strength of steel from 235 MPa to 420 MPa, the ultimate flexure load of the square CFST beam was found to increase. The developed models were also analyzed under cyclic loading condition.

An artificial neural network prediction model was developed to predict the flexural strength of the CFST models. This study aims to establish a comparison between Multilayer Feed forward - a Multilayer Perceptron network (MLP) with feed forward learning - and a Radial Basis Function Network (RBF). From the results, it was observed that the two types of networks (Multilayer Perceptron and Radial Basis Function) were able to predict the results satisfactorily. However, the Multilayer Perceptron network showed higher accuracy than the radial basis function. The R^2 value of MLP analysis was found to be better than RBF.

Keywords*:* *Concrete Filled Steel Tubes (CFST), Flexural behaviour, Composites, Finite element analysis, High strength concrete, Geopolymer Concrete, Artificial neural network.*

TABLE OF CONTENTS

LIST OF FIGURES

LIST OF TABLES

1. INTRODUCTION

1.1. GENERAL

The concrete-filled steel tubular (CFST) structure offers numerous structural benefits, including high strength and fire resistances, favourable ductility and large energy absorption capacities. There is also no need for the use of shuttering during concrete construction; hence, the construction cost and time are reduced. These advantages have been widely exploited and have led to the extensive use of concrete filled tubular structures in civil engineering structures. Concrete-filled steel tubes (CFST) are widely used in structures to support large compressive loads. It consists of steel tubes that are in-filled with concrete that can delay the local buckling of steel tube under loading.

The forming and stripping costs are reduced because the steel tube acts as stay in place formwork during casting of the concrete, and it laterally confines the infilled concrete. The compressive strength of concrete, ductility of concrete and axial capacity of columns are enhanced. Many types of concrete filling may be used which includes plain concrete, high strength concrete, reinforced concrete, light weight concrete, polymer concrete etc. In recent years, CFST columns are generally adopted to resist compressive strength of more than 60MPa. The cross-section is the key element to enhance the strength of CFST profiles and it controls the three fundamental buckling modes: local, distortion and global.

Rectangular CFST columns are the most commonly used in modern construction. They have higher bearing capacity better plasticity and ductility. Circular CFST columns are bi-axially stressed in the hoop and axial directions. Square CFST columns provide confinement to the concrete infill and in return the concrete infill prevents inward local buckling of the steel tube. Elliptical CFST column are found to have higher rigidity and strength than the steel tubular columns.

Tension and compression stresses occur at different regions according to the loads and load conditions in structural members. It can be seen that the optimum resisting section against these stresses in the same member is the reinforced concrete which has had a composite structures since the 1850s. However, recent studies concerning concrete filled steel tubes (CFST)have become important in the area of structural engineering. Structural members have enough bearing

capacity against internal forces according to dead loads and live loads caused by external effects in normal conditions. However, extra shear forces and moments created by seismic movements or dynamic vibrations during earthquakes force the capacities of members. Conventional reinforced cross sections might be of higher dimensions than required during the design stage because of this.

Concrete filled steel tubes have a high ductility and bearing capacity. This system provides for rapid construction without removing any formwork. Steel members prevent lateral expansion of concrete as seen with stirrups. Steel tube performs both longitudinal and lateral reinforcement as well as it is used in formwork. A concrete core resists axial force, at the same time preventing the buckling of steel in an inward direction on a tube. The use of steel walled composite cross sections is becoming widespread in civil engineering. The main purpose of using CFST members is to provide maximum bearing capacity prior to possible buckling modes. Local buckling is expected in the case of the inadequate confinement effects by steel tube or inadequate concrete core strength in a composite section. The confinement effect is called the radial pressure created by steel tubes. It operates in the same manner as stirrups and alters the buckling mode. Slenderness is also an important effect on the buckling mode determined using the dimensions of member.

Rectangular concrete filled steel tubes (RCFST) and Circular concrete filled steel tubes (CCFST) are being used widely in real civil engineering projects due to their excellent static and earthquake resistant properties, such as high strength, high ductility and large energy absorption capacity. Concrete filled steel tubes (CFST) are also used extensively in other modern civil engineering applications. When they are used as structural columns, especially in high-rise buildings, the composite members may be subjected to high shearing force as well as moments under wind or seismic actions. It may be noted here that mechanical and economic benefits can be achieved if CFST columns are constructed taking advantages of high-strength materials. For example, high-strength concrete infill contributes greater damping and stiffness to CFST columns compare to normal strength concrete. Moreover, high-strength CFST columns require a smaller cross-section to withstand the load, which is appreciated by architects and building engineers.

1.2. COMPOSITE ACTION OF CFSTs

The composite action between the steel tube and infill concrete is developed due to the shear stress transfer between the concrete and steel. The stress transfer can be attained by the natural bond between the steel tube and the infill concrete or by using shear connectors. In general, the bond strength of CFSTs members is low. However, the circular cross sections provide higher bond strength and better confinement than the rectangular or square cross sections. Also, the local buckling will be prevented in the circular section and will be more likely to occur in the rectangular or square shapes, hence the circular cross sections are preferable. In practice, the rectangular and square sections are used more than the circular sections due to the lack of design guidelines for the circular sections and the fact that the design of connections is easier for rectangular or square sections. The AISC (2005) and the ACI (318-08) provide design specifications for steel structures and reinforced concrete buildings respectively. However, there is no unified design code for composite members, while the AISC (2005) and the ACI (318-08) have different expressions for the strength and stiffness of CFSTs members.

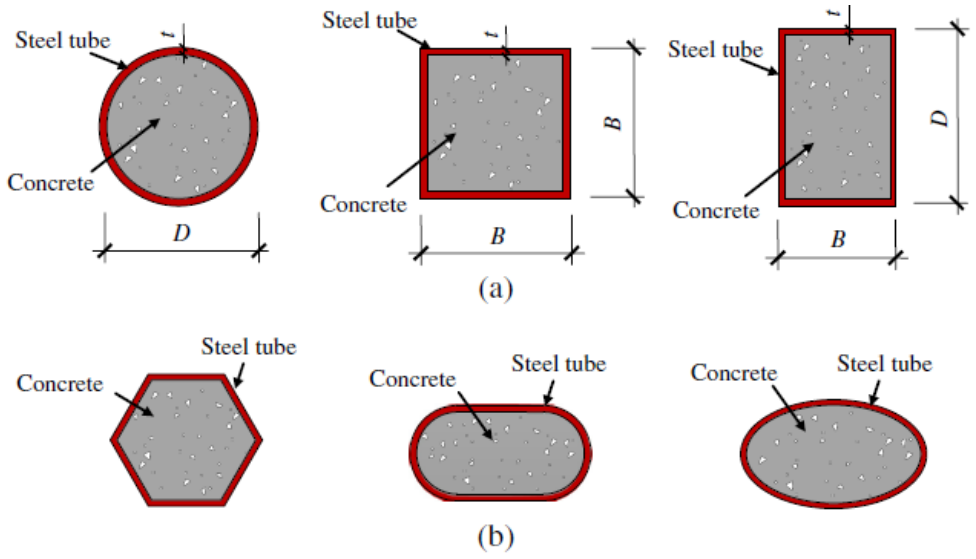

Figure 1. Typical concrete-filled steel tubular cross sections (Source: Lin Hai et al., 2014)

The CFSTs members were developed to combine the prominent characteristics of the steel and concrete and to improve their weak characteristics. In CFSTs, the steel tube will confine the concrete which means increasing its inelastic behaviour and the infill concrete will support the steel tube resulting in improving the local buckling behaviour. **Error! Reference source not found.** presents the effect of the composite behaviour of CFSTs members in terms of axial load

capacity. As explained in the figure, the composite behaviour of CFSTs enhances the axial load capacity of the steel tube and the reinforced concrete member combined. Moreover, the plastic behaviour of the CFST member is also improved compared to the plastic behaviour of the steel tube and reinforced concrete member combined. These results are attributed to the composite action developed between the steel tube and the reinforced concrete member.

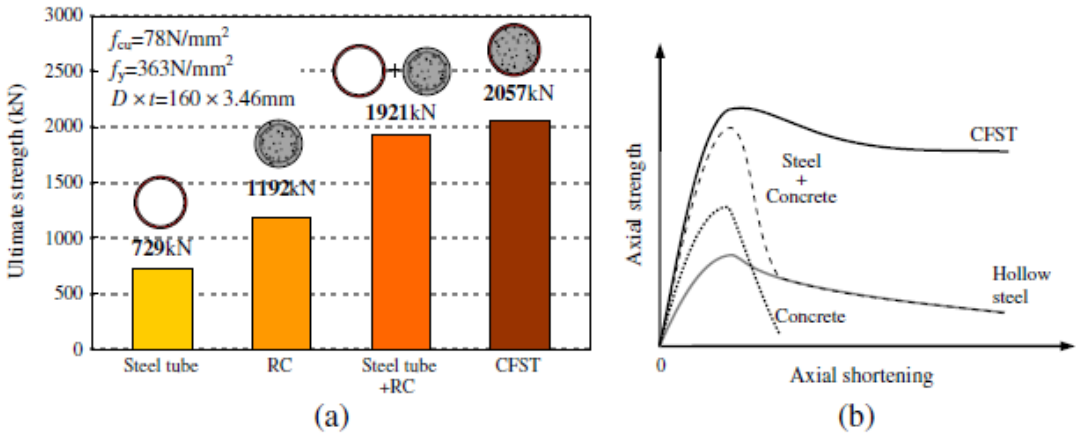

Figure 2: Axial compressive behavior of stub column (Source: Lin Hai et al., 2014)

1.3. ADVANTAGES AND DISADVANTAGES OF CFSTS

The CFSTs has many advantages over the use of bare steel or reinforced concrete members, these advantages can be summarizes as follows:

1. The use of CFSTs members in high rise buildings will result in a smaller cross sections compared with the very large cross sections of the reinforced concrete members that may be needed to fulfill the design requirements.
2. The infill concrete will improve the behavior of the hollow steel section in term of local buckling capacity. Also, inward buckling of the steel tube will not occur due to the support of the infill concrete and thus, only outward local buckling can happen.
3. The construction of the CFSTs members is much easier as the steel tube will act as formwork for casting of the concrete eliminating the need for shuttering. This also means that the construction time and cost will be reduced.

In addition to the advantages of CFSTs, they have some disadvantages such as:

1- Since the steel tube is confining the concrete, the steel will be exposed to air and humidity which make the steel vulnerable to corrosion. Hence, the steel tube need to be painted and maintained continuously.

2- In CFSTs members, the steel is not protected from fire. Therefore, at elevated temperatures the steel strength will decrease significantly.

3- Another important disadvantage of CFSTs members is the lack of sufficient knowledge regarding the bond strength between the infill concrete and the hollow steel section

1.4. SIGNIFICANCE OF THE STUDY

The concrete-filled steel tubular structure can be treated as an alternative system to the steel or the reinforced concrete system. The CFSTs members were developed to combine the prominent characteristics of the steel and concrete and to improve their weak characteristics. In CFSTs, the steel tube will confine the concrete which means increasing its inelastic behaviour and the infill concrete will support the steel tube resulting in improving the local buckling behaviour. The flexural properties of CFST need to be researched more especially with different concrete infills. There is an increasing demand to use sustainable materials like geopolymer concrete. This study focuses on comparing CFSTs filled with high strength concrete and CFSTs filled with geopolymer concrete. In this study, numerical investigations are be carried out to study the behaviour of concrete filled steel tubes having square or rectangular cross-sections. Separate models are used for both high strength concrete and Geopolymer concrete. Thereafter, a parametric study is carried out to evaluate the effect of depth-to thickness ratio, compressive strength of infilled concrete, shear span-to-depth ratio, depth-to-width ratio, and yield strength of steel tube on the flexural behaviour of square and rectangular CFST members.

2. LITERATURE REVIEW

Concrete filled steel tube (CFST) columns have become popular amongst engineers and designers in recent years due to their advantage of having a high compression capacity, good ductility for high seismic resistance, reduction in size of the column, ease of construction and considered high fire resistance **(Zhao et al., 2010).** CFST are used in many structural applications including columns supporting platforms of offshore structures, roofs of storage tanks, bridge piers, piles, and columns in seismic zones. However, due in part to the 1995 Kobe earthquake in Japan, the emphasis on concrete filled steel tube composite column construction was no longer on its structural strength, but rather on its ductility, energy absorption and performance for use in seismic zones **(Kitada, 1998).** Steel tube local buckling is the most critical issue to consider when designing a steel tube column. Therefore, researchers have indicated that addition of concrete infill to the steel tube will reduce the effects of local buckling (**Brauns et al., 1998**).

Among the various materials used, steel fiber reinforced concrete is becoming popular as the use for infill due to its high tensile strength, low shrinkage, high flexural strength, high ductility and energy absorption as indicated by **Ehab and Zhao et al., 2001.** without the physical constraints of having to put longitudinal and transverse reinforcement into the concrete core. Comprehensive experimental and numerical experiments conducted by **Zeghiche & Chaoui, (2005)** and **Johansson & Gylltoft (2001)** respectively, showed that it is possible to achieve ductility in the column by also using high strength concrete. However, it will be more useful to use a thicker steel tube when using a high strength concrete as opposed to normal strength concrete when the ductility of a column is the main concern. **Ehab 2013** concluded that the addition of fiber to plain concrete increases its flexural and tensile strength which results in superior post-elastic material properties. There are various parameters that affect the behaviour of steel fiber reinforced concretes which includes its matrix strength, fiber type, fiber Young's modulus, fiber volume and fiber strength.

Roeder et al. (2016) evaluated the accuracy of using the methods provided by the design codes for determining the flexural strength of circular CFSTs. They collected the data of 122 circular CFSTs specimens, which were tested by previous researchers and compared the moment capacities of the collected data with the design provisions of AISC and ACI. They reported that the plastic stress distribution method given by the AISC specifications gives more reliable results

than the strain compatibility method proposed by both the AISC and ACI specifications. They illustrated that the strain compatibility method significantly underestimates the moment resistance of circular CFSTs and the average ratio between the measured and predicted moment capacity was 1.65, while the average ratio for the plastic stress distribution method was 1.24.

Han et al. (2014) tested a total of 16 concrete filled square hollow sections (SHS) and rectangular hollow sections (RHS) specimens. The length of all specimens was 1100 mm, the depth over width (d/b) ratio was in the range from 1 to 2 and the depth to thickness (h/t) ratio was in the range from 20 to 50. The tubes were made of mild steel plates welded together into a square or rectangular shapes. The concrete used in this experiment was designed to give a compressive strength of 30 MPa at 28 days. From this experimental study, the author was able to determine the maximum moment capacity of the specimens and also investigate the failure pattern after passing the ultimate load. The researcher reported that the failure of the specimens was in a very ductile way. They explained this ductile behavior happens because of the establishment of the composite action between the steel tube and the infill concrete. He illustrated from the moment vs. curvature diagrams that the behavior of the CFSTs is initially elastic, after that, an inelastic behavior occur and the stiffness of the section gradually decrease until the ultimate moment. He defined the ultimate moment capacity of the composite section as the moment corresponding to the maximum steel strain of 0.01 as the moment becomes stable after this value. He also showed that the moment vs. curvature relationship turns to the inelastic stage at 20% of the section's ultimate moment capacity. In addition to the experimental program, the researcher introduced a confinement factor (ξ) to develop a mechanical model that can predict the flexural strength of CFSTs. This factor is equal to $(As * Fy)/(Ac * fc')$ and it was described by the author as a factor that represents the composite action of CFSTs. The author also compared the results of his experimental program with 4 different design codes and his proposed mechanical model. The design codes, which he used, are the AIJ, BS5400, LRFD-AISC and the EuroCode4. He concluded his results by showing that the design codes gave lower moment capacities the than the test results by 10 to 20% and the EuroCode4 and his method were the best to predict the moment capacities.

A further study was made by **Han et al. (2006)** to investigate the flexural behavior of CFSTs using self-consolidating concrete (SCC) instead of normal concrete. They tested a total of 36 beams with circular and square sections, and the parameters they considered are the steel yielding stress (from 235 to 282 MPa), the tube diameter to thickness (d/t), and the shear span to depth ratio a/d (from 1.25

to 6). They stated that in general, the flexural behavior of self-consolidating CFSTs is very similar to those of normal CFSTs. Considering the effect of their parameters on the behavior of beams; they reported that the shear span to depth ratio has no obvious effect on the flexural behavior of CFSTs. They also compared their results with several design codes (AISC, BS5400, AIJ, and Eurocode4) and they found that the moment capacity and the flexural stiffness of self-consolidating CFSTs can be conservatively predicted by these codes.

Moon et al. (2012) developed a nonlinear finite element analysis model that predict the behavior of CFSTs under bending. They reported that the model gave good estimations for the global and local behavior of CFSTs. They conducted parametric studies to select the angle of dilation and friction coefficient between the steel tube and the concrete infill. They recommended an angle of dilation of 20o and a friction coefficient of 0.47 to establish an accurate finite element model for circular CFSTs subjected to flexural loading. Using the FE model, they studied the effects of d/t and fy/fc' ratios on the flexural behavior of CFSTs. They stated that increasing the fy/fc' ratio improved the moment capacity of CFSTs and delayed the local buckling, while the effect of d/t is not significant to the flexural behavior of CFSTs. Furthermore, they compared their results with current design provisions. They indicated that the plastic stress distribution method gives reasonably conservative moment capacity of CFSTs, and the AISC design specifications provide reasonable values for the effective flexural stiffness.

Wang et al. (2015) summarized the flexural behavior of rectangular CFSTs according to previous studies. They mentioned that the parameters were considered are the d/b ratio, the concrete compressive strength, the steel yield stress and the shear span to depth (a/d) ratio. They concluded that the flexural strength of the rectangular CFST section is up to 50% higher than the strength of the bare steel tube section. They also added that the behavior of the rectangular CFST members is very ductile and their mode of failure include outward local buckling of the steel tube at or near the load point, while the infill concrete suffers from flexural cracks at the bottom of the section. They also found from previous studies that the shear span to depth ratio has no significant effect on the flexural behavior of rectangular CFSTs. In order to understand and explain the behavior of rectangular CFSTs, the authors developed a FE model and compared their results with the data of 70 beams tests from previous experimental programs. They found good agreement with the data obtained from tests results in term of the predicted load vs. deformation curves, failure modes and moment capacities. They explained this behavior of rectangular CFSTs by the

composite action or the interaction between the steel tube and the infill concrete as this interaction causes stress redistribution in the steel and concrete which is the main reason of the high moment capacity and ductility.

Bond strength or the bond stress capacity in CFSTs is defined as the stress at the interface when the infill concrete starts to slip. The importance of evaluating the bond stress capacity of CFSTs is very critical in order to enhance the composite action between the steel and concrete and thus improve the structural properties of CFSTs. The bond stress capacity is usually measured by the push-out test. Studies on bond strength using this test have been performed by **Virdi (1980) and Dowling (1993).** They used 104 circular sections with diameters less than 200 and d/t ratios from 15 to 35, they also used 49 rectangular sections. The results showed 3 general trends. First, Concrete strength is not related to the bond strength. Second, the rectangular CFT had lower bond strength than the circular CFT. Finally, the bond strength was decreased by the increase in the diameter and d/t ratio. These studies have agreed that the roughness of the inner surface of the steel tube increases the bond strength of CFSTs, while the use of shear connectors do not affect the bond strength and they only work after the slip of the infill concrete occurs.

According to a study made by **Roeder et al. (2013)** the bond strength in CFSTs depends on the radial displacements resulting from the pressure of wet concrete on the inner surface of the steel tube, the shrinkage of the concrete core and the roughness on the internal surface of the tube. The researchers explained that the bond between the steel tube and infill concrete relies on the interface condition. They mentioned three possible states at the interface, the first state that is called the chemical and mechanical bond is provided by the natural adhesion between the steel and concrete, the interface pressure and the friction coefficient. In the second state, separation between the steel and concrete occurs due to shrinkage of the concrete or the pushing of one material to the other when the load is applied. The third state, which is the common state, is an intermediate one between the first and second state where the adhesion between the steel and concrete is reduced as the separation in the second state starts to appear. The authors conducted an experimental program consists of 20 specimens in order to investigate the bond strength of circular CFSTs. the parameters of the study included the diameter of the concrete, the thickness of the steel tube and the shrinkage of concrete. The steel tubes diameters and the d/t ratio ranged from 250 to 650 mm and 20 to 110 respectively. The shrinkage of concrete was moderate for 8 specimens and was little for 12 specimens. Their results showed that the shrinkage of concrete is a main reason for reducing the

bond strength of CFSTs; they also noticed that tubes with smaller diameters and d/t ratios develop larger bond strength. They recommended using steel tubes with inner irregularities as they significantly increase the bond stress capacity especially for tubes with small diameters and d/t ratios.

Muhammed et al. (2017) in this research, numerical investigations were carried out to study the flexural behavior of square and rectangular CFST members. The predicted load-deformation curves and ultimate moment capacity was found to be in good agreement with experimental results. The FE model was used to investigate the effect of different parameters on the flexural performance of square and rectangular CFST beams. The parameters considered were depth-to-thickness ratio (20−200), compressive strength of infilled concrete (2–100 MPa), shear span-to-depth ratio (1−8), height-to-width ratio (0.6–2), and yield strength of steel tube (380−490). It was found that by changing the depth-to-thickness ratio from 20 to 200 and height-to-width ratio from 0.6 to 2, the ultimate flexural capacity of rectangular CFST increased from 21 to 169 kN-m (up to 8 times) and 46–77 kN-m (67%), respectively. The ultimate capacity also increased (41%) by changing the yield strength of steel tube from 410 to 490 MPa. However, no change in the ultimate moment capacity was observed for different shear span-to-depth ratio (1,3,5,7and 8). Marginal change (up to 11%) in the ultimate capacity was observed by changing the compressive strength of infill concrete from 60 to 100 MPa. Conclusively, the depth-to-thickness ratio and height-to width ratio has significant effect on the ultimate capacity of CFST beams while the effect of shear span-to-depth ratio, strength of infilled concrete and yield strength of steel tube was marginal. Finally, the results from parametric study and previous experimental data available in literature was used to check the accuracy of the existing design methods presented in EC4 (2004), CIDECT, AISC (2010) and GB50936 (2014). It was found that although the closest values were given by GB50936, yet it was not safe to use it for low strength concrete. For all cases, EC 4 was found to be safe but over conservative for square section filled with high-strength concrete, hence, need to be revised.

2.1. OBJECTIVES OF THE STUDY

- Develop a numerical model of CFST beams filled with normal concrete and geopolymer concrete using ANSYS in order to analyze the flexural behavior

- To carry out an extensive parametric study using the verified FE model on the flexural behavior of CFSTs
- Study the flexural behaviour of CFST beams subjected to cyclic loading
- To develop an ANN model to predict the flexural capacity

2.2. SCOPE OF THE STUDY

This study is restricted to the following domains:

- Flexural behaviour of CFST beams
- Analytical study using ANSYS
- Comparative study of two different concrete infill
- Flexural behaviour of CFST beams subjected to cyclic loading
- Prediction of flexural strength using artificial neural network- multilayer perceptron (MLP) & radial basis function (RBF)

3. METHODOLOGY

The methodology employed is discussed below:

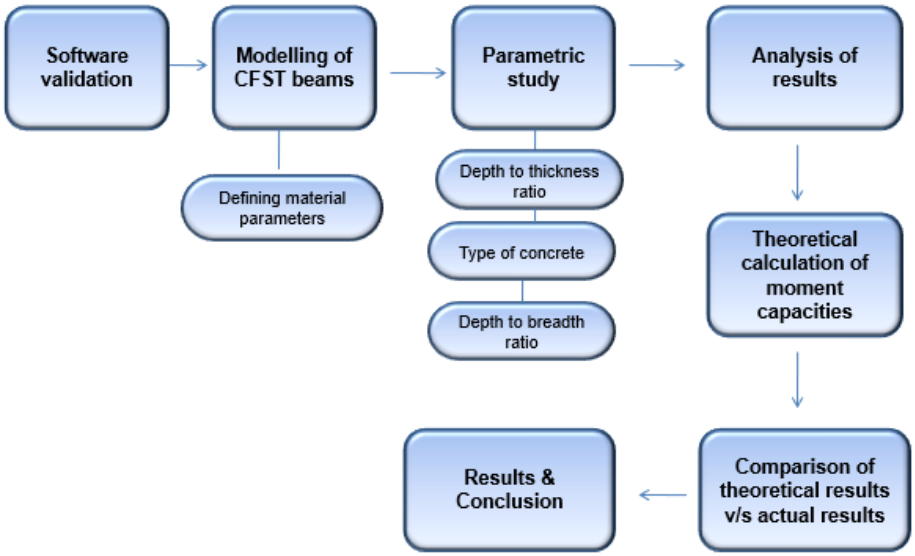

Figure 2*:* Methodology flowchart

A detailed literature review on the concrete filled steel tubes has been done after which the literature gaps, objectives and scope of the study are studied and finalized. As the study progressed, the need for different software for modelling, meshing and doing the FEA became necessary. The modelling of the concrete filled steel tubes is to be done in ANSYS software. For that , the first step is the validation of ANSYS software based on data from the study conducted by Muhammed et al.,(2017). A nonlinear static analysis was conducted. Based on the data from the study, a model was developed. Then a parametric study is conducted by varying the depth to thickness ratio, type of concrete, depth to breadth ratio. Then the models are analyzed under cyclic loading condition. Also, a artificial neural network prediction model was developed to predict the flexural strength of the CFST models. Considering the great potential of this technique, this study aims to establish a comparison between Multilayer Feed forward - a Multilayer Perceptron network (MLP) with feed forward learning and a Radial Basis Function Network (RBF).

3.1. GEOMETRIC MODELLING

ANSYS software is used for finite element modeling to obtain the results. Finite Element Analysis is a mathematical representation of a physical system comprising a part/assembly

(model), material properties, and applicable boundary conditions {collectively referred to as pre-processing}, the solution of that mathematical representation {solving}, and the study of results of that solution {post-processing}. The design is modeled using discrete building blocks called elements. Each element has exact equations that describe how it responds to a certain load. The "sum" of the response of all elements in the model gives the total response of the design. closed form (Exact form), and hence numerical methods are used to obtain solutions.

Structural analysis will be either linear or non-linear. Linear model analysis assumes that the material does not plastically deform (permanent deformation). Non-linear models consist of separating contact conditions (contact with lift-off), when stressing material past its elastic capabilities into the plastic range or bending greater than 10% of model length (large deformation). At this point, material properties change and stresses in the material will vary with the amount of deformation. ANSYS software is divided into different modules where each module has different functions. There is engineering data, geometry, model, setup, solution and results. To create the model, we will need to define the material used – Steel; the geometry of the bar – length and cross-sectional shape and dimensions; the loading – force magnitude and direction; the boundary conditions – the type of support provided and the support locations; and the type of mesh element and the coarseness of the mesh used to analyze the system.

3.2. NON-LINEAR STATIC ANALYSIS

A nonlinear analysis is an analysis where a nonlinear relation holds between applied forces and displacements. Nonlinear effects can originate from geometrical nonlinearity's (i.e., large deformations), material nonlinearity's (i.e., elasto-plastic material), and contact. These effects result in a stiffness matrix which is not constant during the load application. This is opposed to the linear static analysis, where the stiffness matrix remained constant. As a result, a different solving strategy is required for the nonlinear analysis and therefore a different solver. Modern analysis software makes it possible to obtain solutions to nonlinear problems. The source of this nonlinearity can be attributed to multiple system properties, for example, materials, geometry, nonlinear loading and constraints.

3.3. PARAMETRIC STUDY

An extensive parametric study was performed to investigate the influences of depth-to-thickness ratio, type of concrete, depth to breadth ratio on the fundamental behavior of CFST beams under flexure load only. In order to evaluate the individual effect, only one variable will be considered at a time.

3.4. COMPARATIVE STUDY

The comparative study is done based on the modelling results obtained from ANSYS software after finite element modelling. The concrete filled steel tubes with two different types of concrete are modelled and analyzed. Also, the parametric study is done to understand the variation in the models. The results obtained by modelling a square CFST and a rectangular CFST is compared. The CFSTs are filled with high strength concrete and geopolymer concrete. By analyzing the results , the behavior of both the types of CFSTs can be studied.

4. VALIDATION

The Ansys software was validated using the results published by Lin Han et al. (2014). Experimental analysis was conducted to study the flexural behavior of concrete filled steel tubes. A total of 16 concrete-filled steel square hollow sections (SHS) and rectangle hollow sections (RHS) beam specimens were tested. A summary of the specimens is presented in Table 1 where the section sizes and material properties are given. The specimens were designed with a wide range of width-to-depth ratio (from 1 to 2) was achieved. The tube depth to wall thickness ratio ranged from 20 to 50. All the specimens were 1100 mm in length. The tubes were manufactured from mild steel sheet. The tubes with four plates were cut from the sheet, tack welded into a square or rectangular shape and then welded with a single bevel butt weld at the corners. The ends of the steel tubes were cut and machined to the required length. The insides of the tubes were wire brushed to remove any rust and loose debris present. The deposits of grease and oil, if any, were cleaned away. Each tube was welded to a square steel base plate of 10 mm thickness. Strips of the steel tubes were tested in tension in accordance with the Chinese standard related to metal materials. Three coupons were taken from each of the steel sheets: from these tests, the average yield strength of the steel tube (f_{sy}). The modulus of elasticity of the tubes was found to be approximately 200,000 MPa. A type of concrete, with a compressive cube strength (f_{cu}) at 28 days of 30 MPa, was designed.

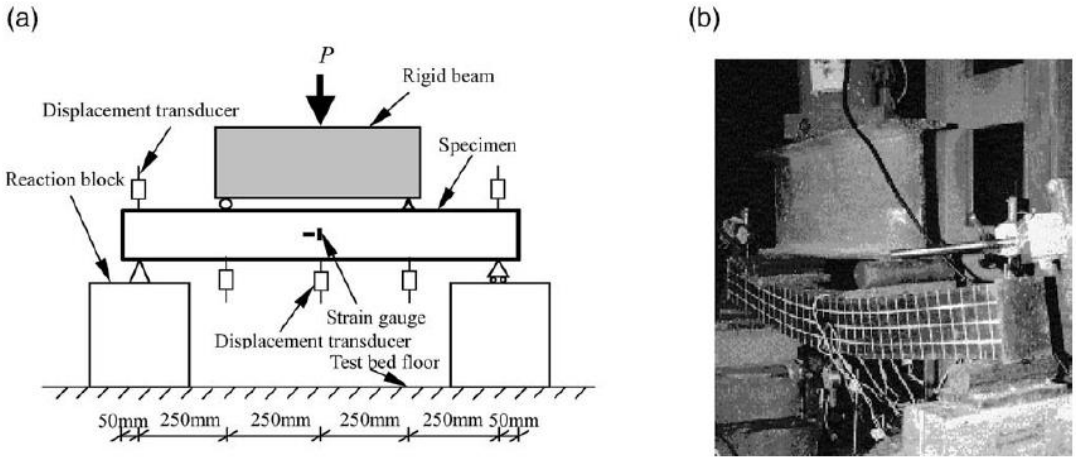

Figure 3. Arrangement of beam test (Source: Lin Hain et al., 2014)

A four-point bending rig was used to apply the moment. The in-plane displacements were measured at locations along the specimen by three displacement transducers. Eight strain gauges

were used for each specimen to measure strains at the mid-span. Figure 3 gives a general view of the test setup. A load interval of less than one-tenth of the estimated load capacity was used. Each load interval was maintained for about 2–3 min. At each load increment, the strain readings and the deflection measurements were recorded. All specimens were loaded to failure. The structural behavior of a square CFST beams filled with normal strength concrete was investigated using nonlinear FE models in ANSYS software. In nonlinear analysis, the convergence is more easily achieved by using displacement-controlled load. Hence, for all cases, displacement-controlled load was applied. The displacement was slowly increased until the ultimate capacity of the beam was reached.

The structural steel was assumed to have isotropic hardening behavior, so that yield stresses increase or decrease in all stress directions when plastic straining occurs. The modulus of elasticity and the Poisson's ratio for the steel were taken as 2×10^5 MPa and 0.3, respectively. A surface-based interaction with a Coulomb friction model in the tangential direction and hard contact pressure model in the normal direction was used to model the interface between steel and concrete core. The friction factor in all the models was taken as 0.6. The ANSYS FE software provides various types of elements that could be used to model the steel, concrete and interface between steel and concrete. For this research, the steel tube was modelled using 3D hexahedral reduced integration solid element and concrete was modelled using 3D quadrilateral reduced integration solid element. Adequate size and number of elements were selected by performing mesh convergence study on some models.

Table 4.1: Details of the specimen used for verification of FE model of normal strength CFST

Sample Name	B*D*t (mm)	L (mm)	f_c (MPa)	f_y (MPa)	E_s (MPa)
RB1-1	120*120*3.84	1100	27.3	330.1	200,000

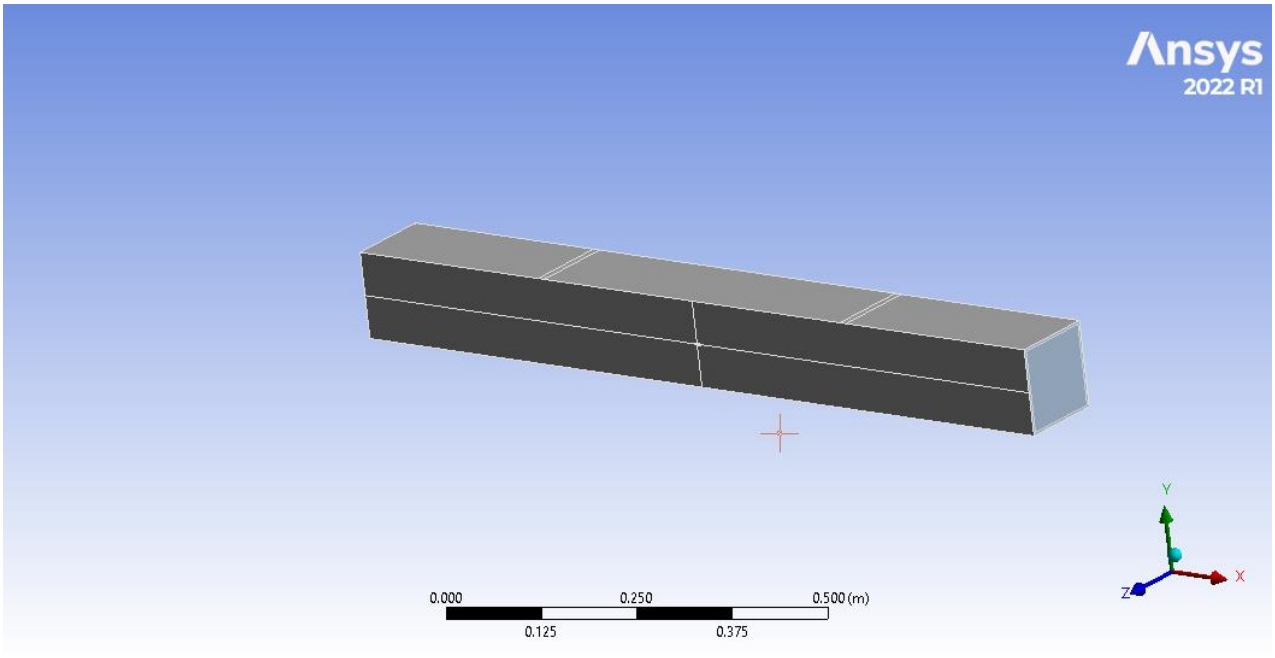

Figure 4. CFST beam modelled using ANSYS software

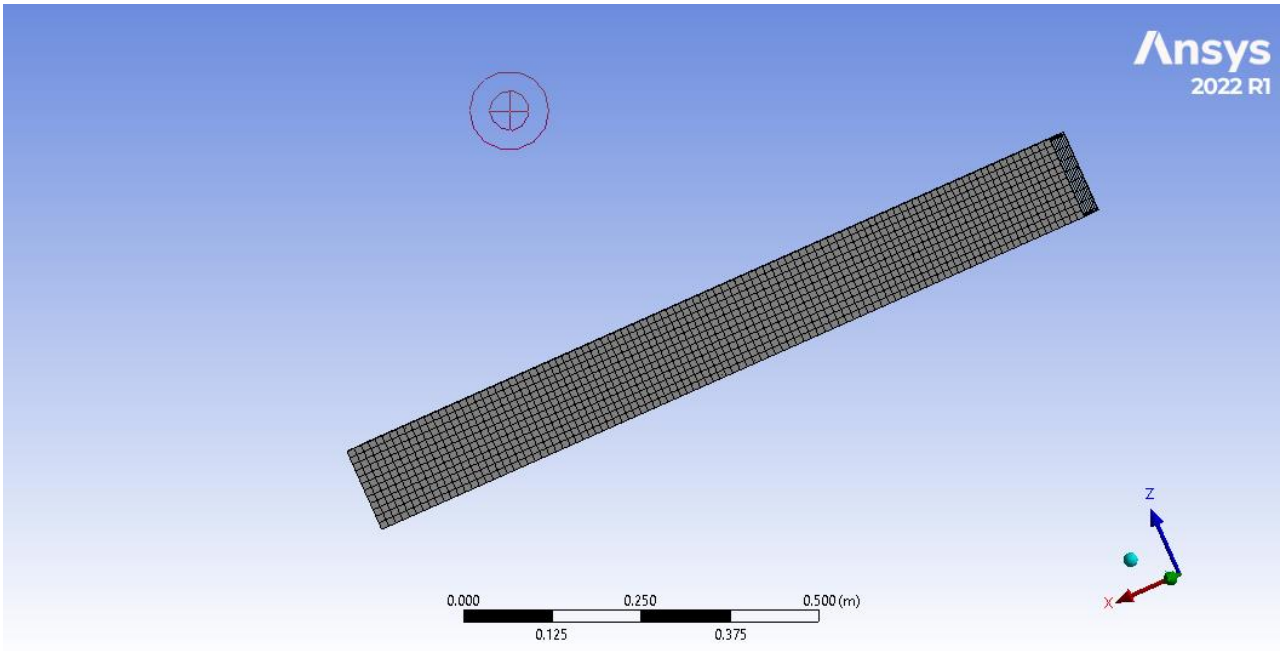

Figure 5. Meshed model

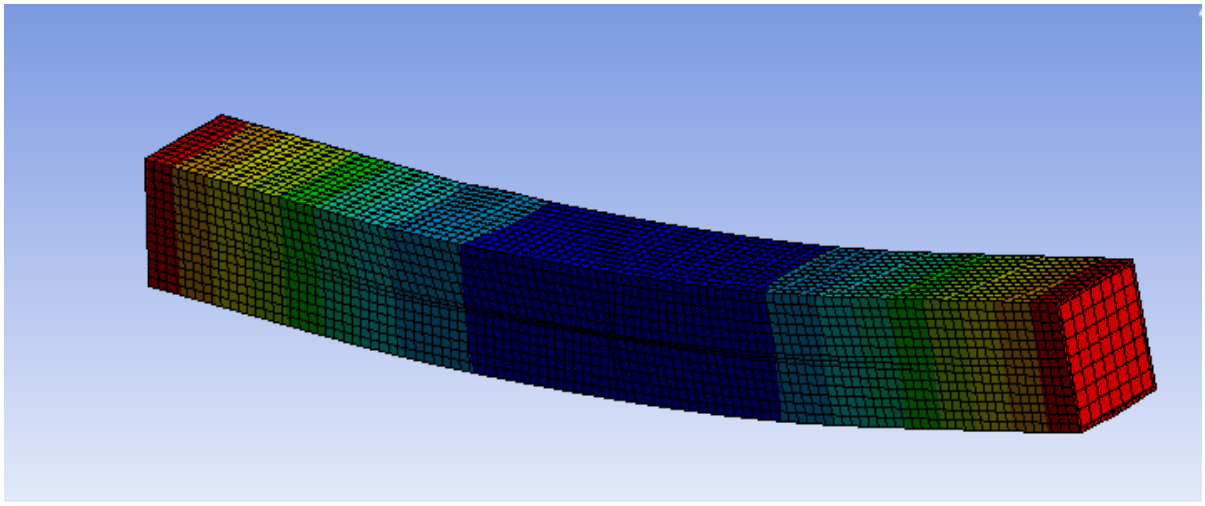

Figure 6. Deformed model

Figure 6 shows the graph comparing experimental results published and finite element results obtained. The comparison of mid-span deflection between FE model and experimental specimen RB1-1 tested by Lin Han et al., (2014). The results show that FE model predicts accurately the load-deflection curve up to ultimate load. However, some deviation from the experimental load-deflection curve occurs due to the uncertainty in material properties and some unknown assumptions made due to the lack of data availability.

4.1. RESULTS AND DISCUSSION

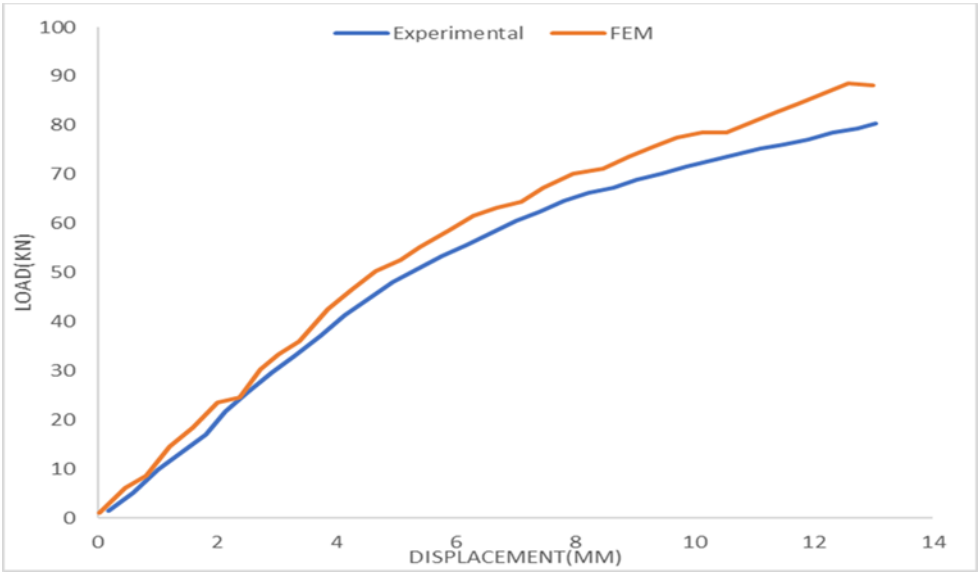

Figure 7. Load deflection curve comparison of experimental and FE model

Table 4.2: Comparison of ultimate load and displacement values

Parameters	From experimental analysis	FE modelling	Percentage variation
Ultimate Load (kN)	80.32	88.05	9.62%
Displacement (mm)	13.04	11.95	8.3%

The ultimate load value and displacement value from the numerical analysis and experimental analysis are tabulated above in table 4.2. A variation of 9.62% and 8.3% are observed in the ultimate load and displacement values respectively. Since the variation is less than 10% the software and model can be used for analysis. However, some deviation from the experimental load-deflection curve occurs due to the uncertainty in material properties and some unknown assumptions made due to the lack of data availability.

5. NUMERICAL INVESTIGATION

5.1. MODELLING OF CFST FILLED WITH HIGH STRENGTH CONCRETE

The detailed numerical study was done in ANSYS. Four basic models of CFST. Square and rectangle CFST filled with high strength concrete and geopolymer concrete was made. A square CFST filled with geopolymer concrete and a rectangular CFST filled with geopolymer concrete. The structural behavior of a square and rectangular CFST beams filled with high strength concrete and geopolymer concrete was investigated using nonlinear FE models in ANSYS software. In non-linear analysis, the convergence is more easily achieved by using displacement-controlled load. Hence, for all cases, displacement-controlled load was applied. The displacement was slowly increased until the ultimate capacity of the beam was reached.

Table 5.1: Material Properties of CFST filled with high strength concrete

Shape	B×D×t (mm)	L(mm)	fc (MPa)	fy(MPa)	Es(MPa)
Square	120×120×3.84	1200	60.9	330.1	36480
Rectangle	150×120×2.93	1200	60.9	330.1	36480

The material properties of CFST with high strength concrete is given in the table 5.1. The Poisson's ratio is taken as 0.3 for steel and 0.2 for concrete. The Drucker Prager (DP) model was used for modelling the concrete. The concrete plasticity model of Drucker-Prager (DP) was employed to describe the behavior of confined concrete. The uniaxial compressive strength was taken as 60.9 MPa, uniaxial tensile strength as 4.1MPa , and biaxial compressive strength as 70.6 MPa. The contacts between the concrete core and the steel tubes and the plates were defined as frictional with the friction coefficient of 0.5. The value of fiction coefficient was defined based on the literature review. The core concrete was model using first-order hex elements of the type SOLID 185. The CFST filled with geopolymer was modelled using the stress-strain curve obtained from Saranya et al., (2019). A surface-based interaction with a Coulomb friction model in the tangential direction and hard contact pressure model in the normal direction was used to model the interface between steel and concrete core. The friction factor in all the models was taken as 0.6. The ANSYS FE software provides various types of elements that could be used to model the steel,

concrete and interface between steel and concrete. The details of the loading setup (two-point loading conditions) and the mesh used for square and rectangular CFST beams are given in figure 4 .Adequate size and number of elements were selected by performing mesh convergence study on some models. The mesh size for steel was taken as 10mm and for steel as 15mm.

5.1.1. MODELLING OF SQUARE CFST FILLED WITH HIGH STRENGTH CONCRETE

The modelling of square CFST filled with high strength concrete is given below. Fig 9 shows the CFST beam modelled using ANSYS. Fig 10 shows the meshed model and fig 11 shows the deformed model.

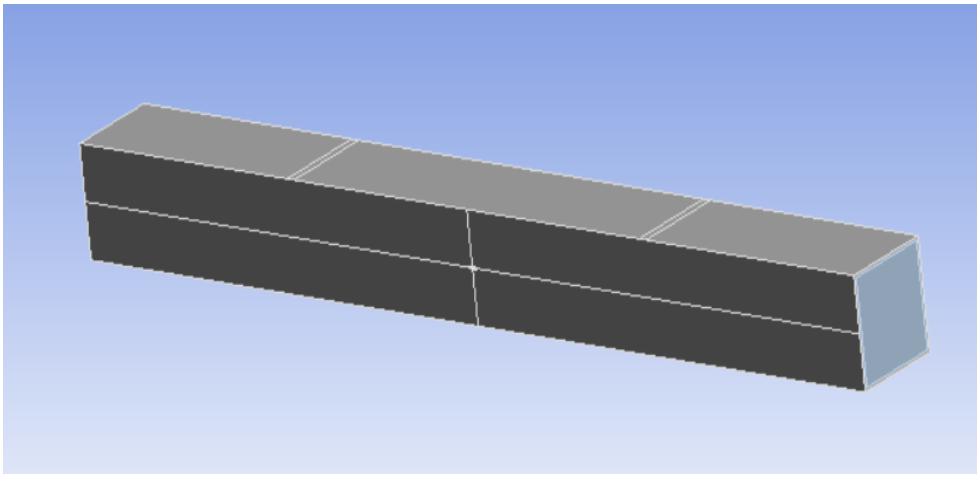

Figure 9 : CFST beam modelled using ANSYS

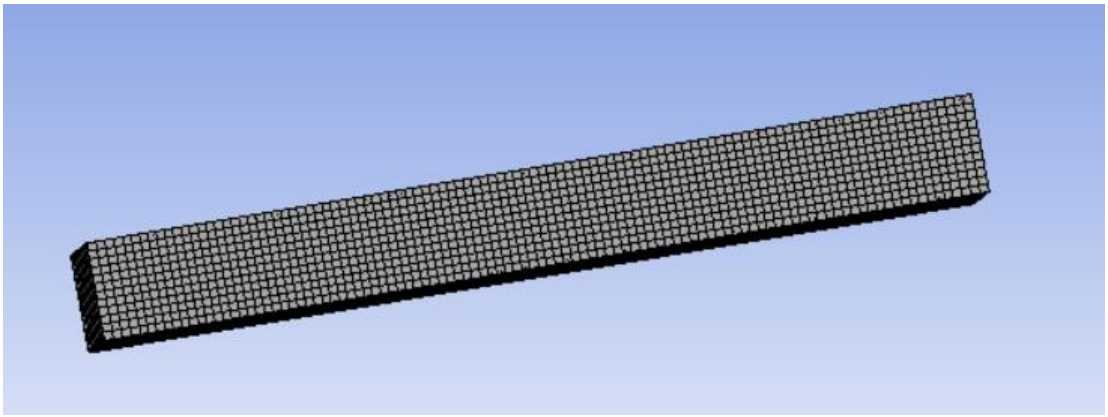

Fig 10: Meshed Model

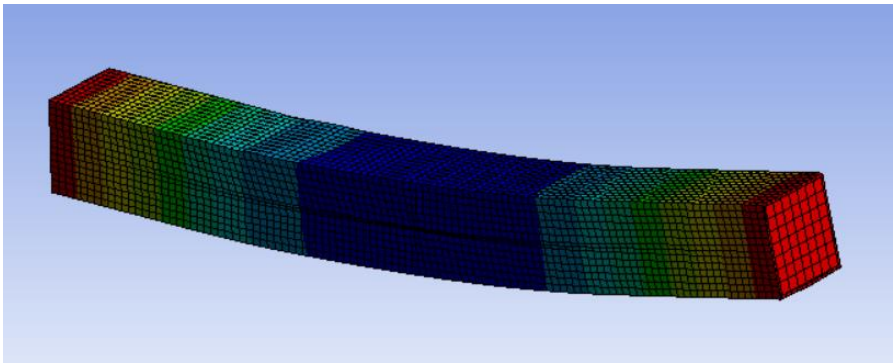

Fig 11: Deformed Model

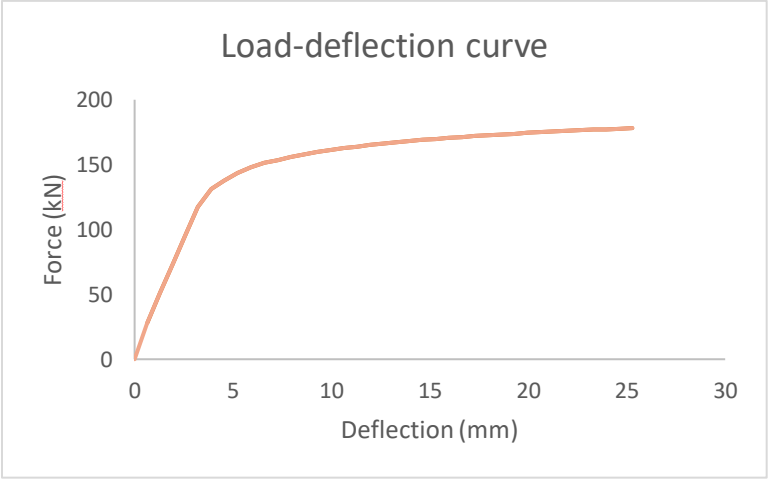

Fig12: Load Deflection curve of CFST filled with high strength concrete

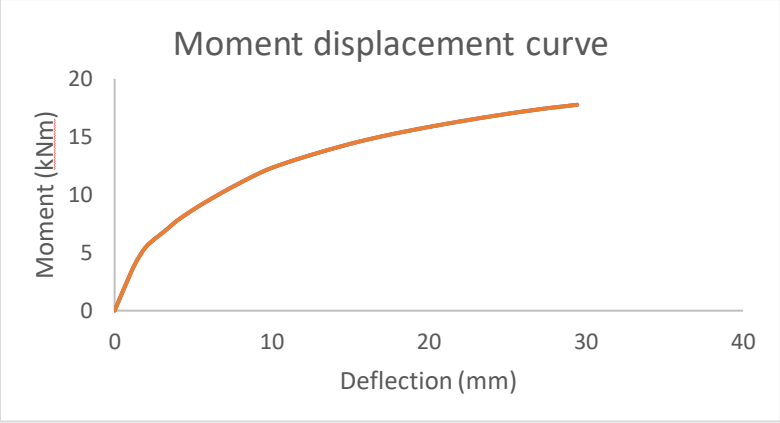

Fig13: Moment Deflection curve of CFST filled with high strength concrete

The results of the analysis the square CFST filled with high strength concrete is given in the above fig 12 and fig 13. The maximum load value obtained was 178 kN with a deflection of 25.1 mm. The moment obtained was 17.2 kN with a deflection of 29.6mm.

5.1.2. MODELLING OF RECTANGULAR CFST FILLED WITH HIGH STRENGTH CONCRETE

The modelling of square CFST filled with high strength concrete is given below. Fig 14 shows the CFST beam modelled using ANSYS. Fig 15 shows the meshed model and fig 16 shows the deformed model

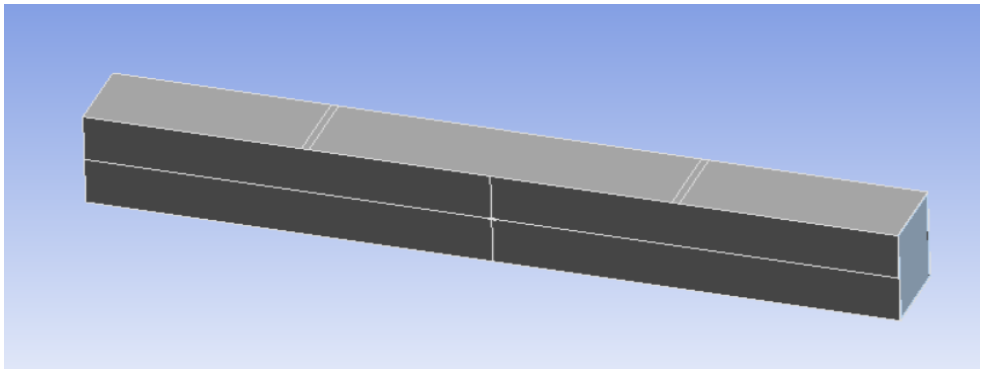

Fig 14 : CFST beam modelled using ANSYS

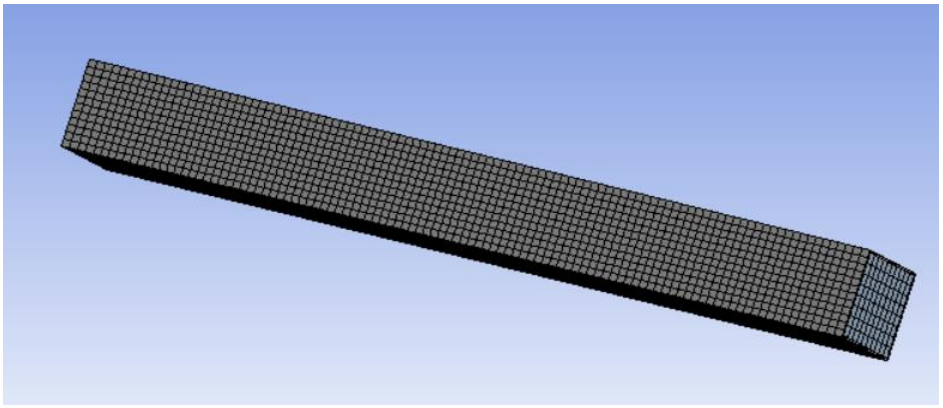

Fig 15: Meshed Model

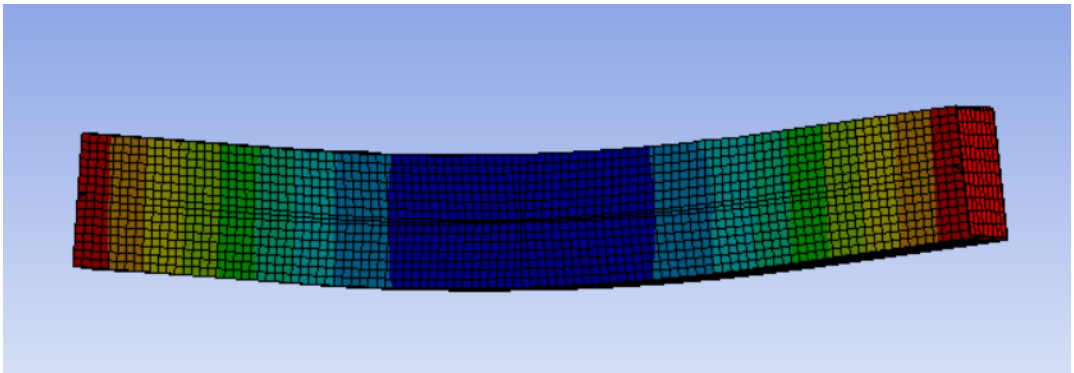

Fig 16: Deformed model

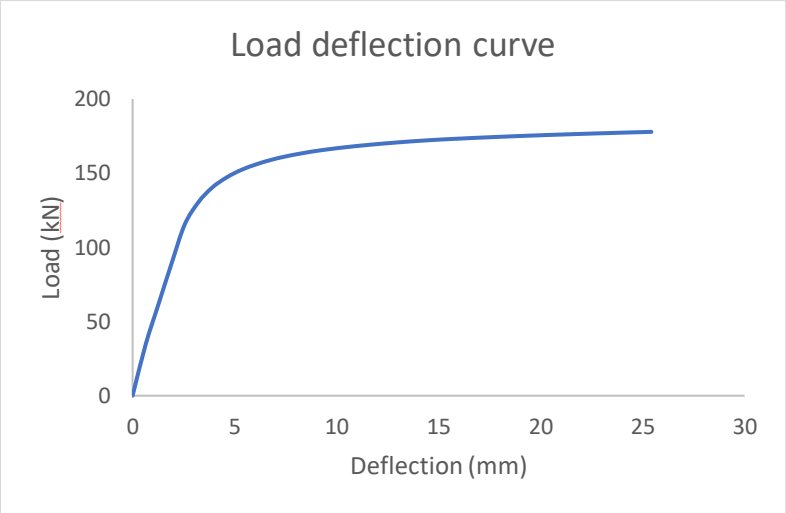

Fig 17: Load Deflection curve

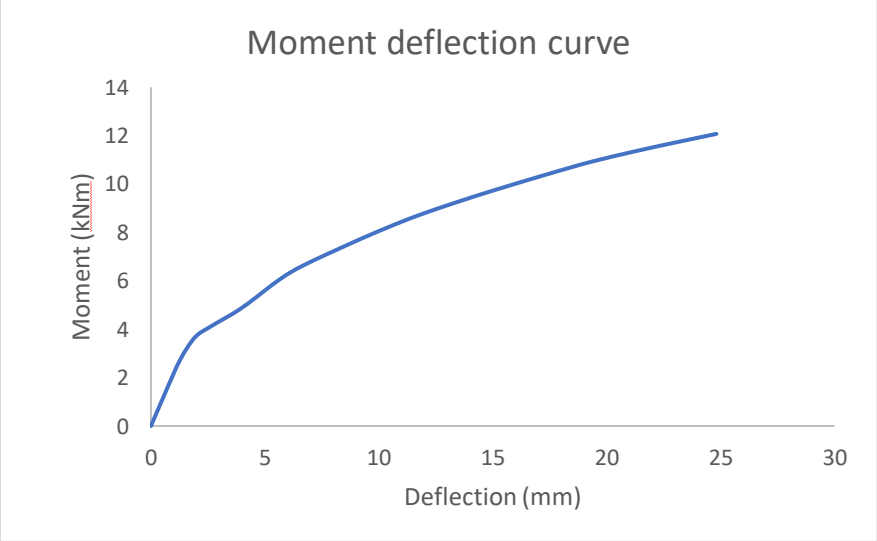

Fig 18: Moment Deflection curve

The results of the analysis the square CFST filled with high strength concrete is given in the above fig 17 and fig 18. The maximum load value obtained was 177.2 kN with a deflection of 24.9 mm. The moment obtained was 12.4 kN with a deflection of 24.2 mm.

5.2. MODELLING OF CFST FILLED WITH GEOPOLYMER CONCRETE

A square CFST filled with geopolymer concrete and a rectangular CFST filled with geopolymer concrete was modelled in ANSYS. The structural behavior of a square and rectangular CFST beams filled with high strength concrete and geopolymer concrete was investigated using nonlinear FE models in ANSYS software. In non-linear analysis, the convergence is more easily achieved by using displacement-controlled load. Hence, for all cases, displacement-controlled load was applied. The displacement was slowly increased until the ultimate capacity of the beam was reached.

Table 5.2: Material Properties of CFST filled with high strength concrete

Shape	B×D×t(mm)	L(mm)	Poisson's ratio	fy(MPa)	Es(MPa)
Square	120×120×3.84	1200	0.2	330.1	38600
Rectangle	150×120×2.93	1200	0.2	330.1	38600

The material properties of CFST with high strength concrete is given in the table 5.2. The Poisson's ratio is taken as 0.3 for steel and 0.2 for concrete. The Drucker Prager (DP) model is used for modelling the concrete. The concrete plasticity model of Drucker-Prager (DP) was employed to describe the behavior of confined concrete. The stress-strain curve of geopolymer concrete used for the analysis is given below.

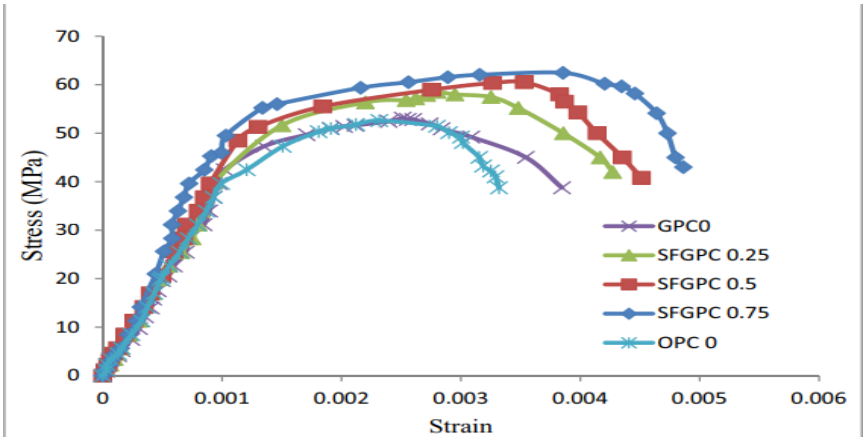

Fig 19: Stress strain graph of geopolymer concrete (Saranya et al., (2019)

The contacts between the concrete core and the steel tubes and the plates were defined as frictional with the friction coefficient of 0.5. The value of fiction coefficient was defined based on the literature review. The core concrete was model using first-order hex elements of the type SOLID 185. The CFST filled with geopolymer was modelled using the stress-strain curve obtained from Saranya et al., (2019) . A surface-based interaction with a Coulomb friction model in the tangential direction and hard contact pressure model in the normal direction was used to model the interface between steel and concrete core. The friction factor in all the models was taken as 0.6. The ANSYS FE software provides various types of elements that could be used to model the steel, concrete and interface between steel and concrete. The details of the loading setup (two-point loading conditions) and the mesh used for square and rectangular CFST beams are shown in Figs. 20 and 21. Adequate size and number of elements were selected by performing mesh convergence study on some models. The mesh size for steel was taken as 10mm and for steel as 15mm.

5.2.1. MODELLING OF SQUARE CFST FILLED WITH GEOPOLYMER CONCRETE

The modelling of square CFST filled with high strength concrete is given below. Fig 20 shows the CFST beam modelled using ANSYS. Fig 21 shows the meshed model and fig 22 shows the deformed model.

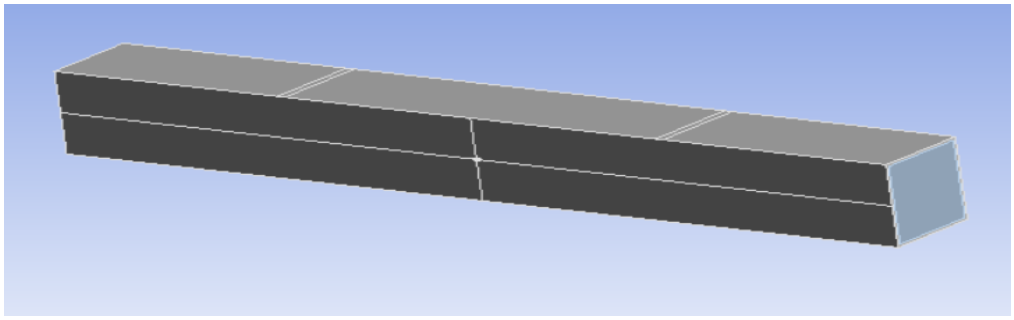

Fig 20 : CFST beam modelled using ANSYS

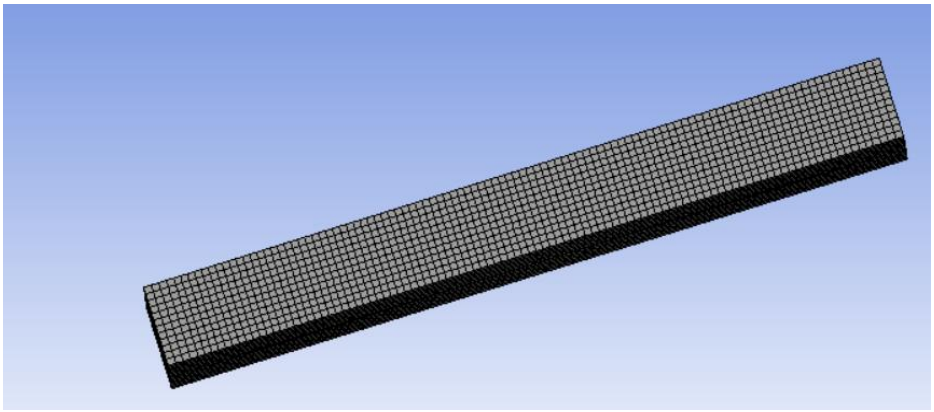

Fig 21: Meshed Model

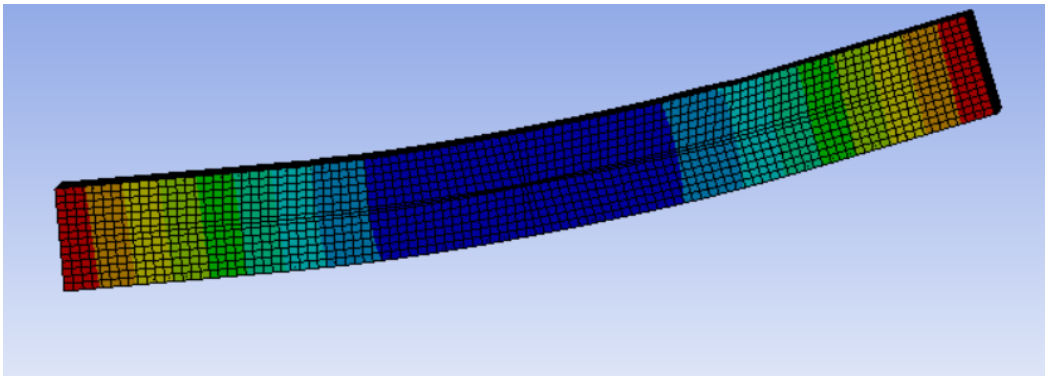

Fig 22: Deformed model

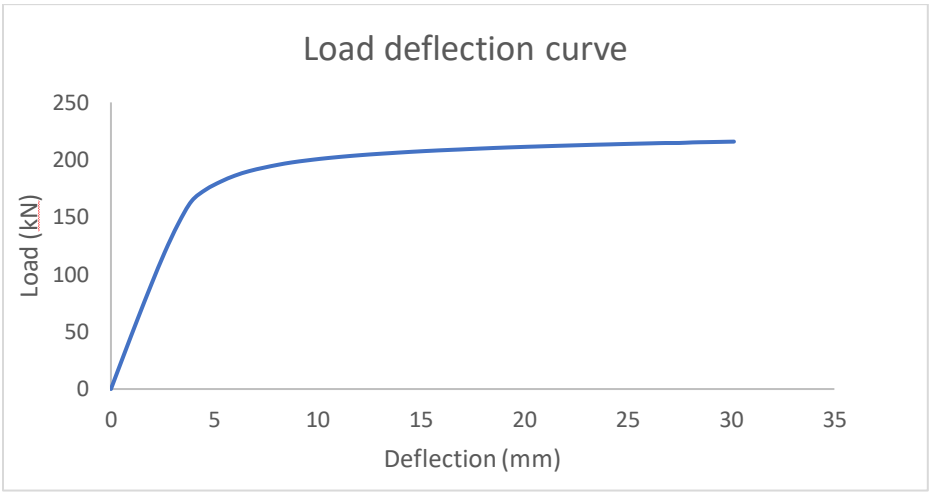

Fig 23: Load deflection curve

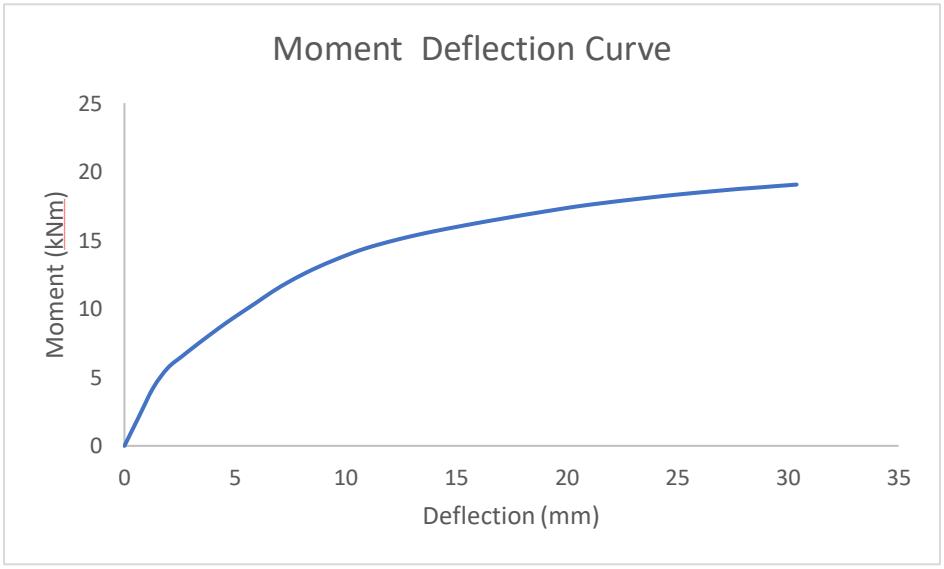

Fig 24: Moment deflection curve

The results of the analysis the square CFST filled with geopolymer concrete is given in the above fig 23 and fig 24. The maximum load value obtained was 215.2 kN with a deflection of 30.2 mm. The moment obtained was 19.2 kN with a deflection of 30.1 mm.

5.2.2. MODELLING OF RECTANGULAR CFST FILLED WITH GEOPOLYMER CONCRETE

The modelling of square CFST filled with high strength concrete is given below. Fig 25 shows the CFST beam modelled using ANSYS. Fig 26 shows the meshed model and fig 27 shows the deformed model.

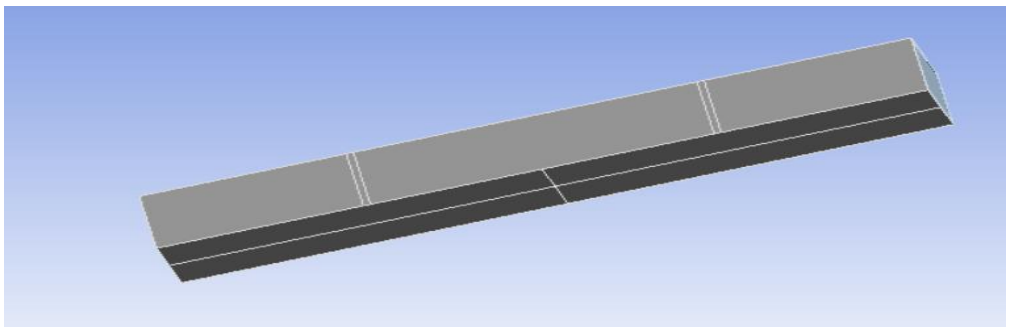

Fig 25 : CSFT beam modelled using ANSYS

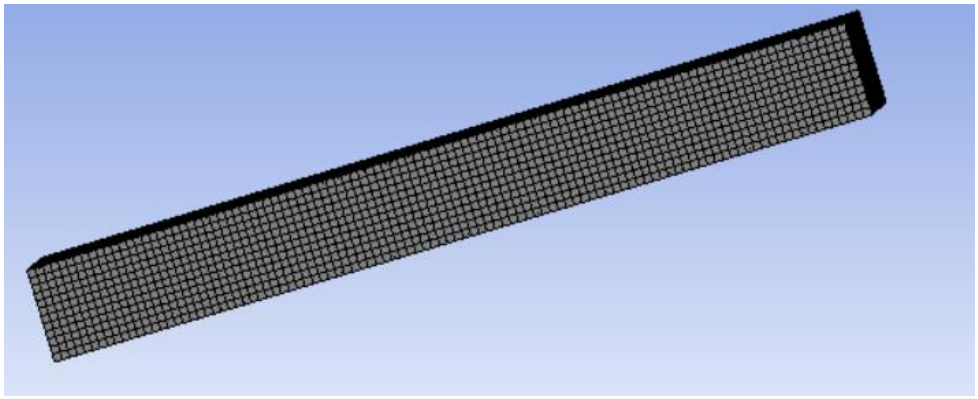

Fig 26: Meshed Model

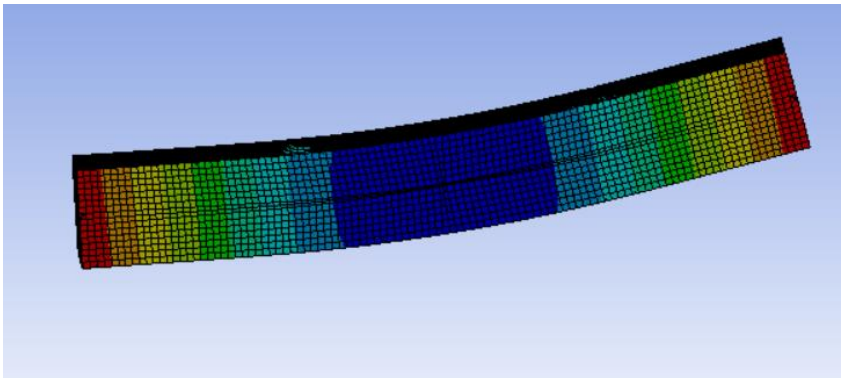

Fig 27: Deformed model

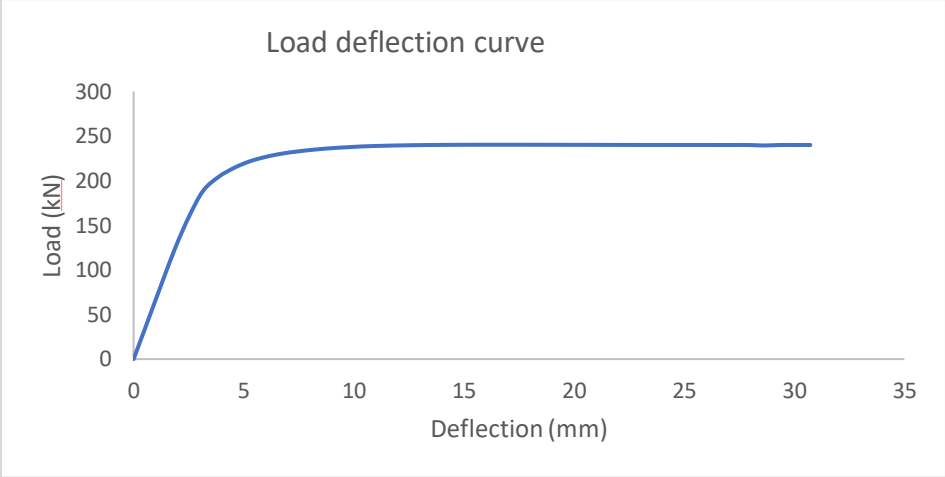

Fig 28: Load Deflection curve

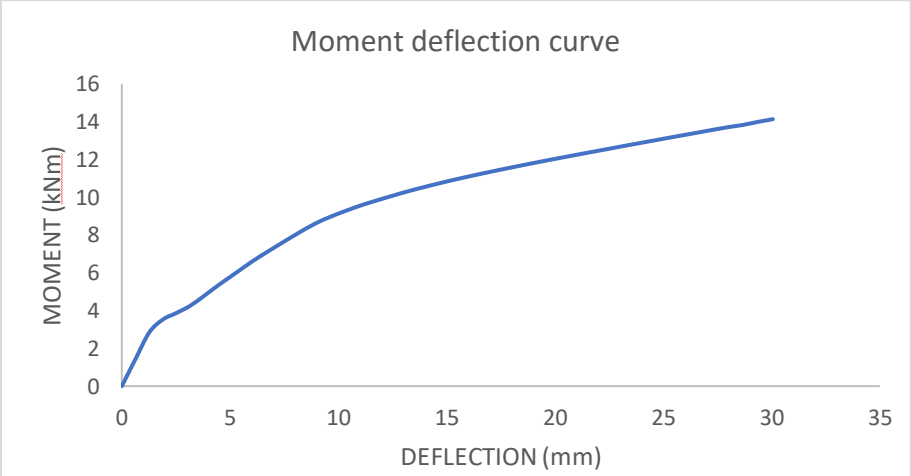

Fig 29: Moment deflection curve

The results of the analysis the square CFST filled with geopolymer concrete is given in the above fig 28 and fig 29. The maximum load value obtained was 240.2 kN with a deflection of 30.1 mm. The moment obtained was 14.2 kN with a deflection of 30.06 mm.

5.3. PARAMETRIC STUDY

An extensive parametric study was performed to investigate the influences of depth-to-thickness ratio (28.57−200), effect of D/B ratio (24-42.8) and steel yield strengths (235–420 MPa) on the fundamental behavior of CFST beams under flexure load only. In order to evaluate the

individual effect, only one variable was considered at a time. For parametric study, the length of the beam was kept as 1200 mm.

5.3.1. CFST SQUARE SECTION FILLED WITH HIGH STRENGTH CONCRETE & GEOPOLYMER CONCRETE - EFFECT TO DEPTH THICKNESS RATIO IN SQUARE BEAMS

The main objective of this parametric study was to evaluate the effects of different Depth-to-thickness ratio (D/t) of CFST beams on its structural behavior and ultimate bending moment capacity. For this purpose, four different D/t ratios in the range of 200-28.57 were selected. The D/t ratio was changed by increasing the thickness of the steel tube. In order to represent the behavior of square beams, the Depth-to-width (D/B) ratio of four samples was kept as 1 while for rectangular beams; the D/B ratio of the remaining 4 samples was kept as 2. The detailed dimensions and designations of the FE model are presented in Table 5.3 while the rest of the parameters and boundary conditions were same as mentioned earlier. Multilinear isotropic hardening properties for geopolymer concrete were given from literature – Praveen et al.,(2019).

Table 5.3: Dimension of square CFST

B×D×t (mm)	D/t	D/B
200×200×1	200	1
200×200×3	66.66	1
200×200×5	40	1
200×200×7	28.57	1

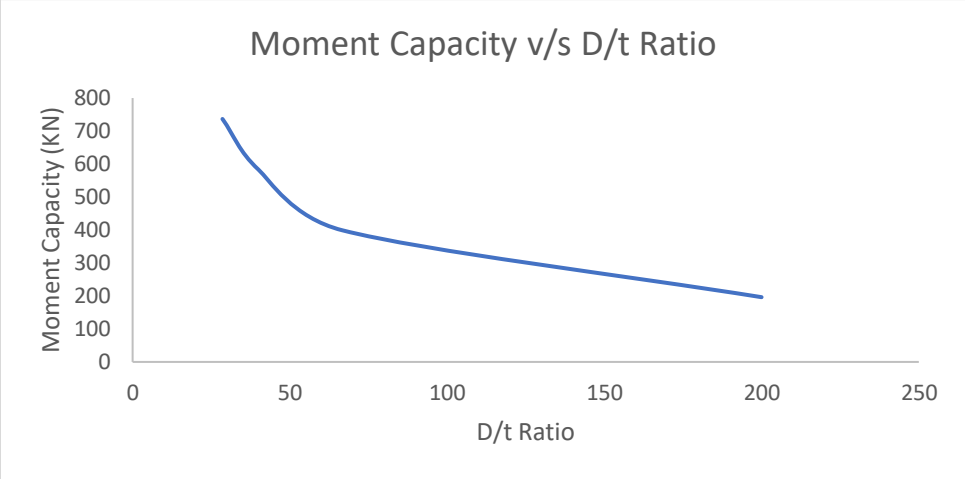

Fig 30**:** Moment Capacity v/s D/t ratio of square CFST filled with high strength concrete

The influence of D/t ratio of CFST on the flexure capacity for square CFST beam filled with high strength concrete is illustrated in Fig. 30. It can be seen that by increasing D/t ratio from 28.57 to 200 (7 times), the ultimate bending moment capacity reduced from 207.8 to 21 kN-m (almost 8 times) for square CFST beams. The reduction in ultimate bending moment capacity is attributed to the fact that the beam having larger D/t ratio has a lesser area of steel. Furthermore, based on beams B/t and D/t ratios, they are categorized in different codes as compact and non-compact. The beams having higher D/t ratios are categorized as non-compact and may fail due to local buckling, which reduces the ultimate load carrying capacity of the beam.

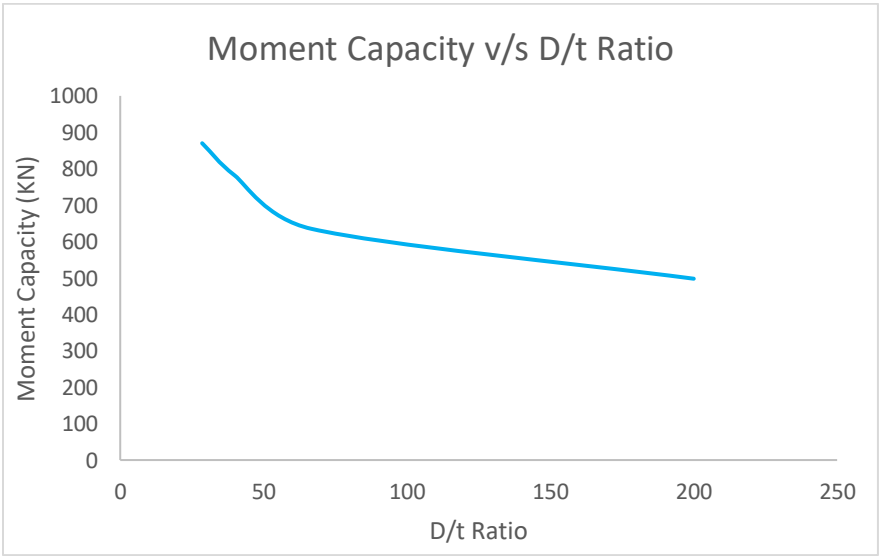

Fig 31: Moment Capacity v/s D/t ratio of square CFST filled with geopolymer concrete

5.3.2. CFST RECTANGLE SECTION FILLED WITH HIGH STRENGTH CONCRETE & GEOPOLYMER CONCRETE - EFFECT OF DEPTH TO THICKNESS RATIO IN RECTANGULAR BEAMS

Four different D/t ratios in the range of 200-28.57 were selected. The D/t ratio was changed by increasing the thickness of the steel tube. In order to represent the behavior of square beams, the Depth-to-width (D/B) ratio of four samples was kept as 1 while for rectangular beams; the D/B ratio of the remaining 4 samples was kept as 2. The detailed dimensions and designations of the FE model are presented in Table 5.4 while the rest of the parameters and boundary conditions were same as mentioned earlier.

Table 5.4. Dimensions of rectangular CFST

B×D×t (mm)	**D/t**	**D/B**
100×200×1	200	2
100×200×3	66.66	2
100×200×5	40	2
100×200×7	28.57	2

The influence of D/t ratio of CFST on the flexure capacity for rectangular CFST beam filled with high strength concrete is illustrated in Fig. 32. It can be seen that by increasing D/t ratio from 28.57 to 200 (7 times), the ultimate bending moment capacity reduced from 207.8 to 21 kN-m (almost 8 times) for square CFST beams. The reduction in ultimate bending moment capacity is attributed to the fact that the beam having larger D/t ratio has a lesser area of steel. Furthermore, based on beams B/t and D/t ratios, they are categorized in different codes as compact and non-compact.

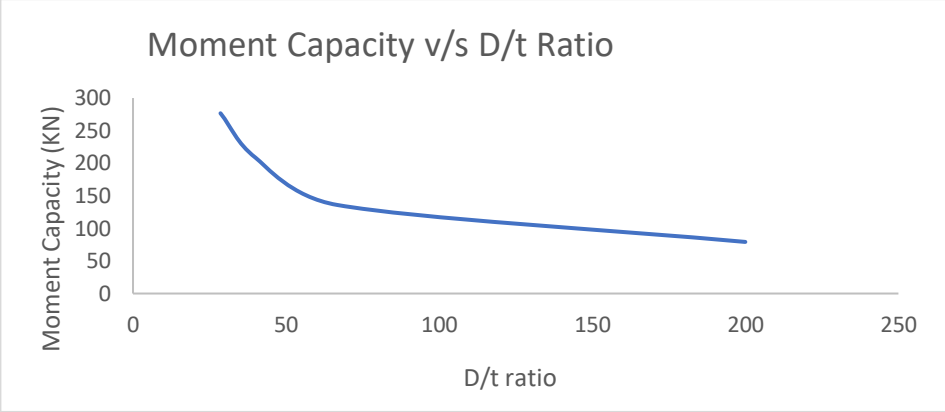

Fig 32: Moment Capacity v/s D/t ratio of rectangle CFST filled with high strength concrete

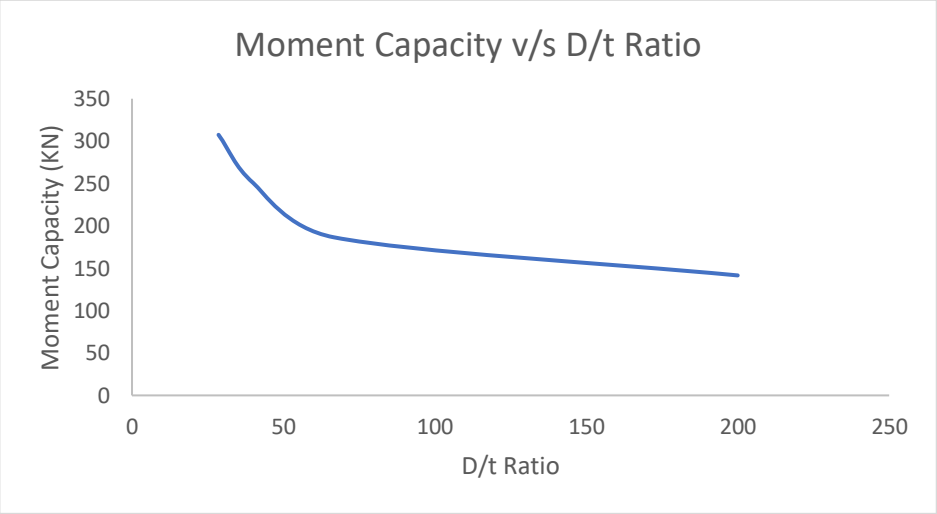

Fig 33: Moment Capacity v/s D/t ratio of rectangle CFST filled with geopolymer concrete

5.3.3. CFST SQUARE SECTION FILLED WITH HIGH STRENGTH CONCRETE & GEOPOLYMER CONCRETE - INFLUENCES OF STEEL YIELD STRENGTH IN SQUARE BEAMS

The square and rectangular CFST beams with different steel yield strengths and with same D/t ratio of 40 were analyzed. The loading conditions and length of the beam were same as mentioned in previous section. The rest of the parameters along with ultimate moment capacity are given in Table 5.5. The yield strength of steel was increased from 235 MPa to 420 MPa .

Table 5.5. Material properties of square CFST

B×D×t (mm)	fy (MPa)	D/t
200×200×5	235	40
200×200×5	345	40
200×200×5	390	40
200×200×5	420	40

Fig. 34 illustrates the influence of steel yield strengths on the ultimate moment capacity of square beams. The ultimate flexure strength of square CFST beams was found to increase significantly with an increase in the yield strength of steel. By increasing the yield strength of steel from 235 MPa to 420 MPa, the ultimate flexure load of the square CFST beam was found to increase from 20.45 KNm to 28.99 KNm .

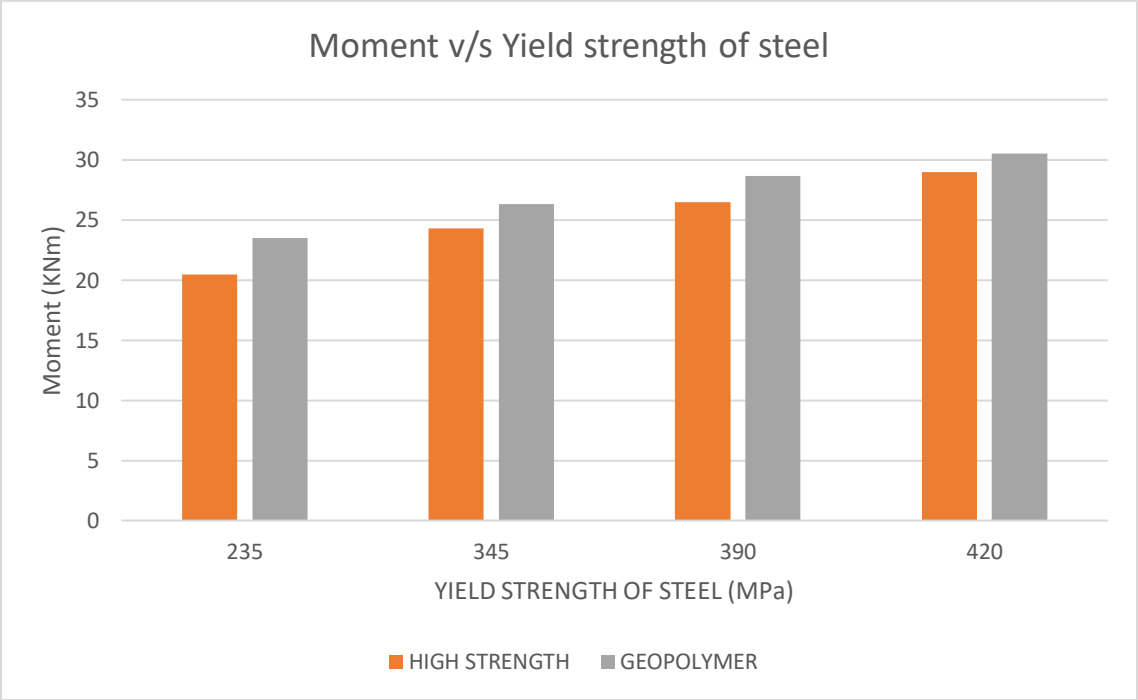

Fig 34 : Moment v/s yield strength of steel of square CFST

5.3.4. CFST SQUARE SECTION FILLED WITH HIGH STRENGTH CONCRETE & GEOPOLYMER CONCRETE INFLUENCES OF STEEL YIELD STRENGTH IN RECTANGULAR BEAMS

The rectangle CFST beams with different steel yield strengths and with same D/t ratio of 40 were analyzed. The rectangular CFST beams also showed similar behavior.

Table 5.6. Material properties

B×D×t (mm)	fy (MPa)	D/t
100×200×5	235	40
100×200×5	345	40
100×200×5	390	40
100×200×5	420	40

Fig. 34 illustrates the influence of steel yield strengths on the ultimate moment capacity of rectangle beams. The ultimate flexure strength of square CFST beams was found to increase significantly with an increase in the yield strength of steel. By increasing the yield strength of steel from 235 MPa to 420 MPa, the ultimate flexure load of the square CFST beam was found to increase from 17.7 KNm to 29.2 KNm.

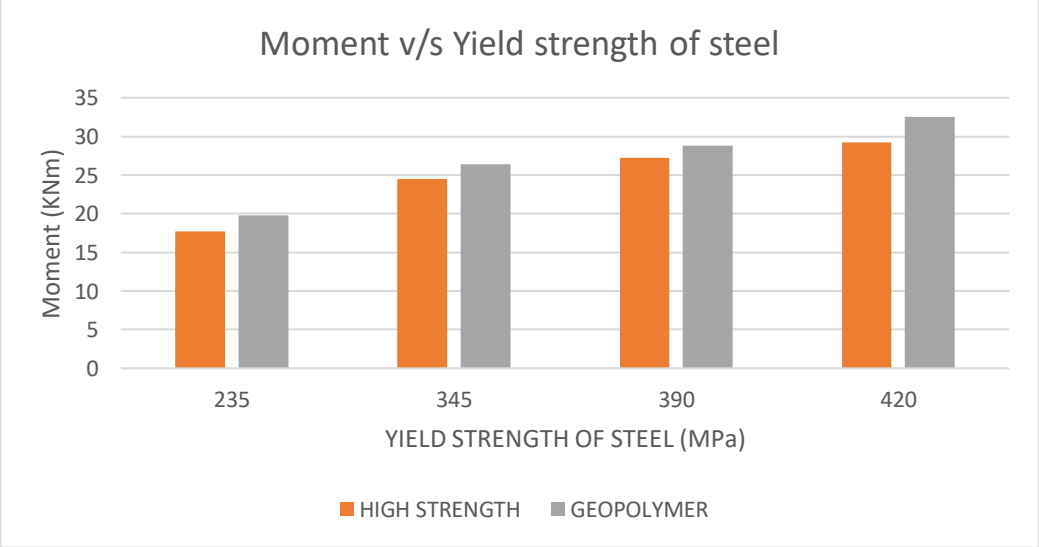

Fig 35: Moment v/s yield strength of steel of rectangle CFST

5.3.5. CFST SECTION FILLED WITH HIGH STRENGTH CONCRETE & GEOPOLYMER CONCRETE- EFFECT OF D/B RATIO

The ultimate bending strength of CFST beams depends on Depth-to width (D/B) ratio. Hence, the effect of D/B ratio on the ultimate moment/load capacity and load deflection curves of CFST beams were determined. The dimensions of the beams were selected in such a manner that the total amount of steel remains constant. For this purpose, the width and depth of steel tubes were only changed. The calculated values of D/B ratios of the beam sections were 0.54 ,0.7, 1, 1.67 and 2. The CFST filled with high strength concrete as well as geopolymer concrete was used for the analysis. Further details are given in Table 5.7.

Table 5.7: Dimensions of the CFSTs

B×D×t (mm)	**D/t**	**D/B**
220×120×5	24	0.54
200×140×5	28	0.7
160×160×5	32	1
120×200×5	40	1.67
107×214×5	42.8	2

The influence of D/B ratio of CFST steel tube on the ultimate bending moment capacity of CFST beams is shown in Fig.36. Irrespective of the value of compressive strength, the ultimate flexural capacity of beam increased significantly with the increase in D/B ratio. This is attributed to the fact that the beam having larger D/B ratio has a large moment of inertia and have high resistance to local and global buckling, which in turn, increased the ultimate load carrying capacity of the beam. When the D/B ratio increased from 0.54 to 2, the ultimate capacity of members is increased by more than 50%.

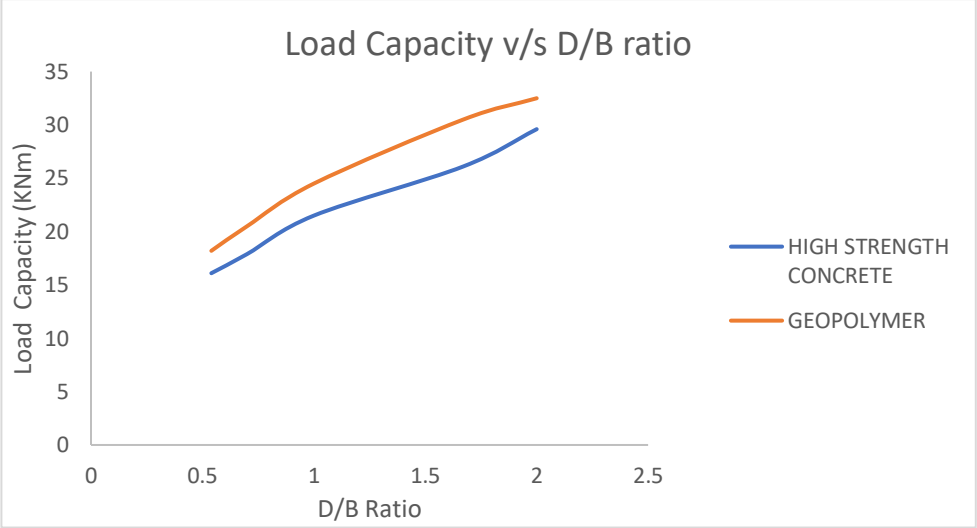

Fig 36: Load capacity v/s D/B ratio

5.4. NUMERICAL ANALYSIS OF CFST BEAMS UNDER CYCLIC LOADING

The numerical analysis of CFST under cyclic loading was done in ANSYS. Four basic models of CFST were made. A square CSFT filled with high strength concrete and a rectangle filled with high strength concrete. It was followed by changing the concrete infill to geopolymer concrete. A square CFST filled with geopolymer concrete and a rectangular CFST filled with geopolymer concrete.

Table 5.8: Material Properties

Shape	B×D×t (mm)	L(mm)	fc (MPa)	fy (MPa)	Es (MPa)
Square	120×120×3.84	1200	60.9	330.1	36480
Rectangle	150×120×2.93	1200	60.9	330.1	36480

The material properties of CFST with high strength concrete is given in the table 5.8. The Poisson's ratio is taken as 0.3 for steel and 0.2 for concrete. The Drucker Prager (DP) model is used for modelling the concrete. The concrete plasticity model of Drucker-Prager (DP) was employed to describe the behavior of confined concrete. The uniaxial compressive strength was taken as 60.9 MPa, uniaxial tensile strength as 4.1MPa , and biaxial compressive strength as 70.6 MPa. The contacts between the concrete core and the steel tubes and the plates were defined as frictional with the friction coefficient of 0.5. The value of fiction coefficient was defined based on the literature review. The core concrete was model using first-order hex elements of the type

SOLID 185. The CFST filled with geopolymer was modelled using the stress-strain curve obtained from Saranya et al., (2019). A surface-based interaction with a Coulomb friction model in the tangential direction and hard contact pressure model in the normal direction was used to model the interface between steel and concrete core. The friction factor in all the models was taken as 0.6. The ANSYS FE software provides various types of elements that could be used to model the steel, concrete and interface between steel and concrete. Cyclic loading was given to the beam specimens in such a manner that specimens were loaded to a pattern such as -5,5, -10,10, -15,15..and so on .

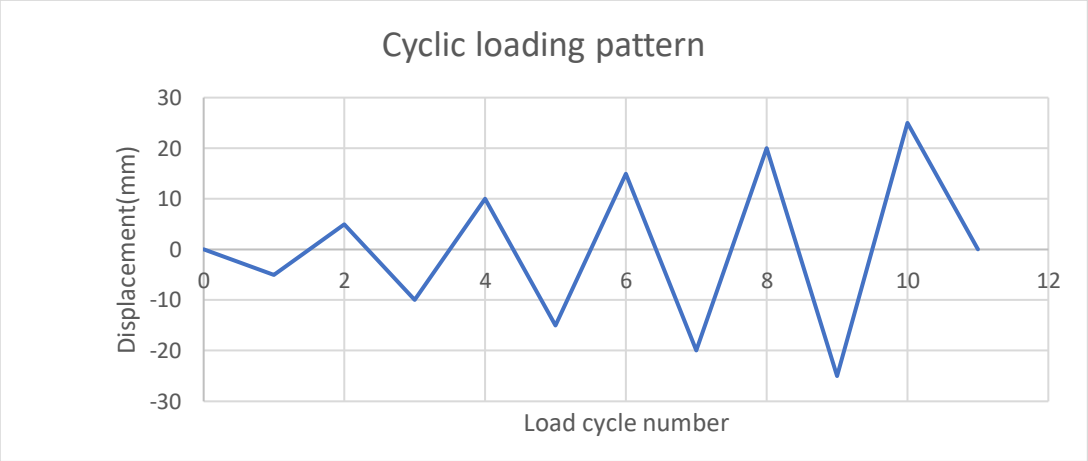

Fig 37: Cyclic loading pattern for beam

5.4.1. MODELLING OF SQUARE CFST FILLED WITH HIGH STRENGTH CONCRETE

The modelling of square CFST filled with high strength concrete is given below. Fig 38 shows the CFST beam modelled using ANSYS. Fig 39 shows the meshed model and fig 40 shows the deformed model.

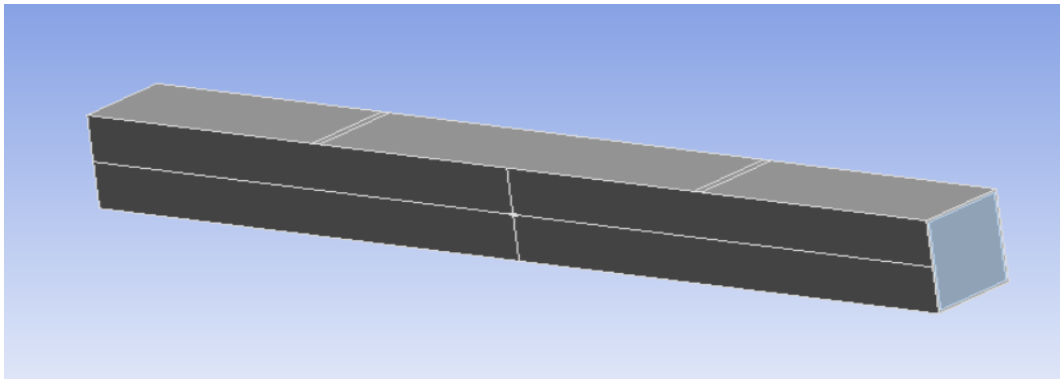

Fig 38: CFST beam modelled using ANSYS

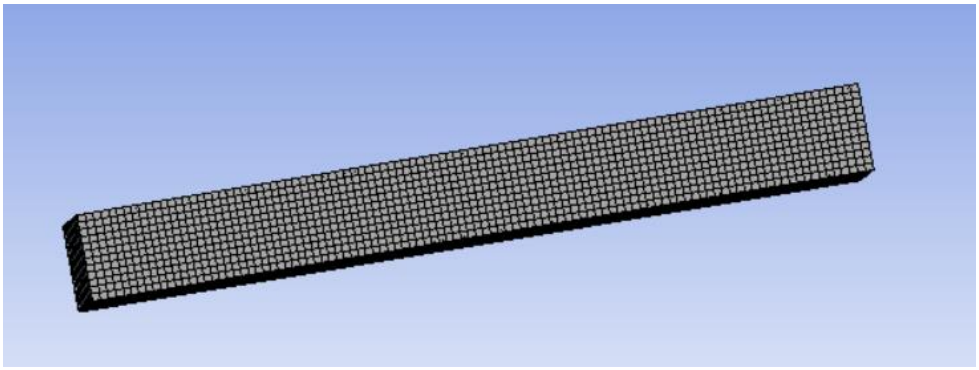

Fig 39: Meshed Model

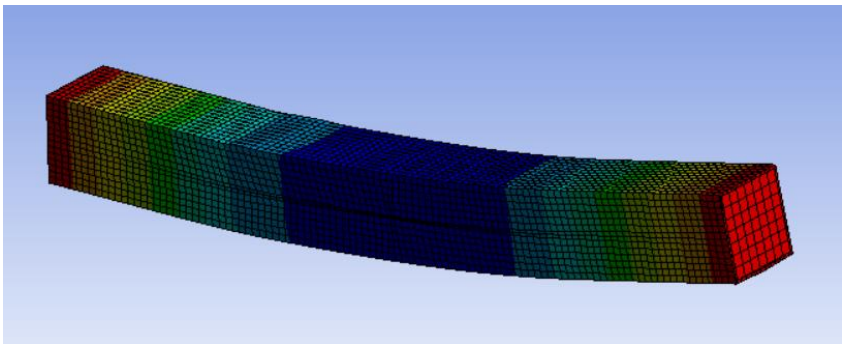

Fig 40:Deformed Model

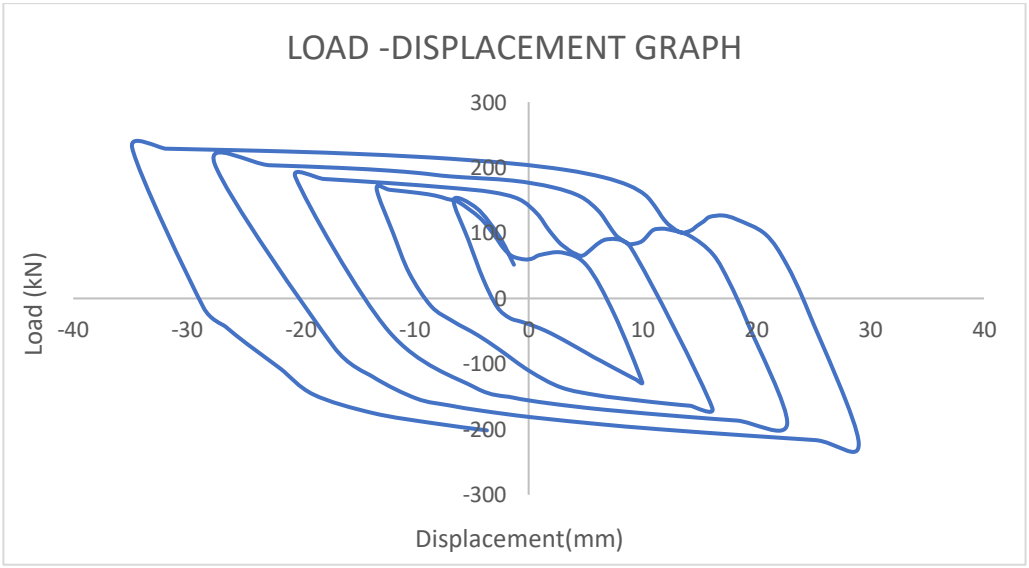

Fig 41: Load deflection curve

The results of the analysis the square CFST filled with high strength concrete under cyclic loading is given in the above fig 41. The maximum load value obtained was 220.1 kN with a deflection of 28.22mm.

5.4.2. MODELLING OF RECTANGLE CFST FILLED WITH HIGH STRENGTH CONCRETE

The modelling of rectangle CFST filled with high strength concrete is given below. Fig 42 shows the CFST beam modelled using ANSYS. Fig 43 shows the meshed model and fig 44 shows the deformed model.

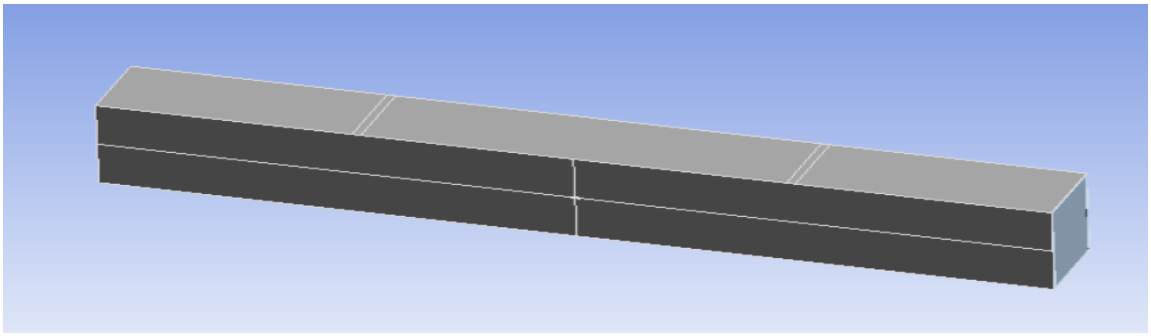

Fig 42: CFST beam modelled using ANSYS

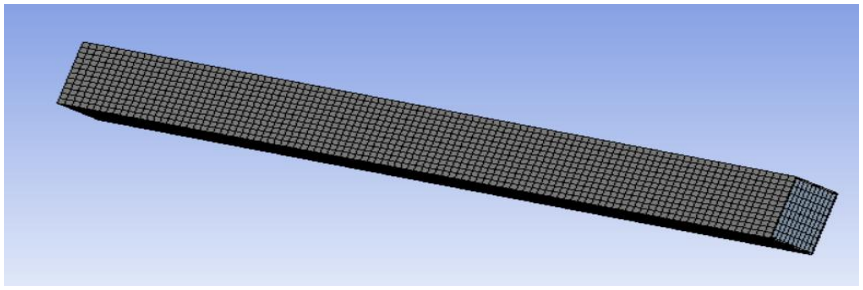

Fig 43:Meshed model

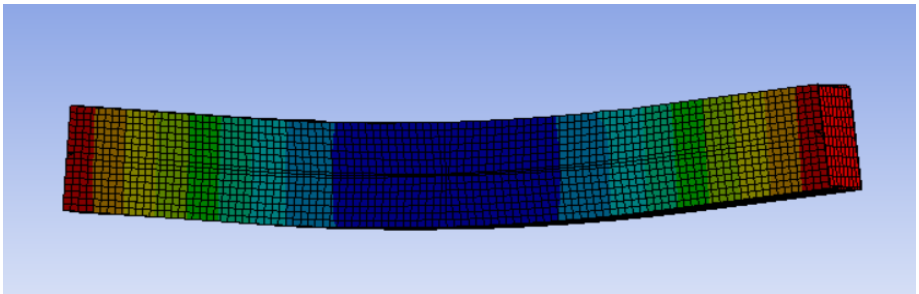

Fig 44: Deformed model

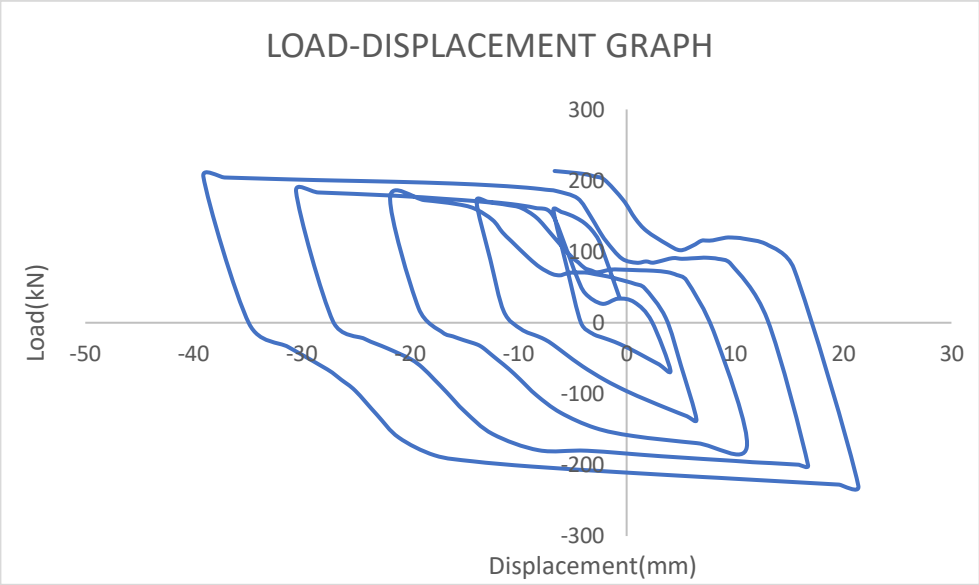

Fig 45: Load deflection curve

The results of the analysis the rectangle CFST filled with high strength concrete under cyclic loading is given in the above fig 45. The maximum load value obtained was 229.12 kN with a deflection of 21.4 mm.

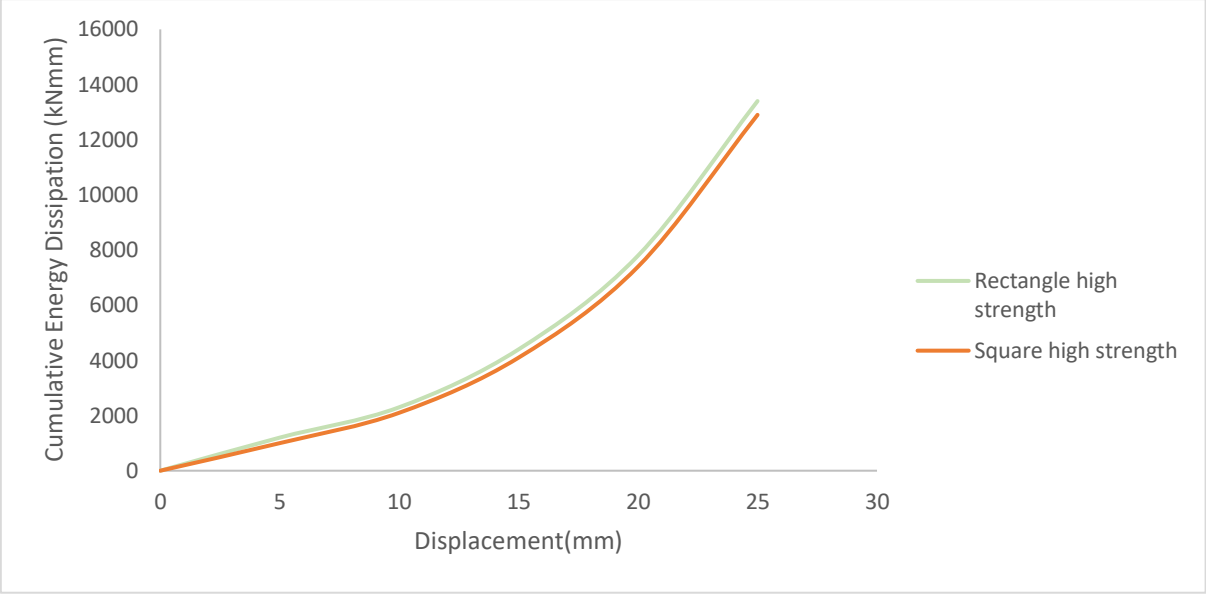

Fig 46: Cumulative energy dissipation – displacement curve

5.4.3. MODELLING OF SQUARE CSFT FILLED WITH GEOPOLYMER CONCRETE

The modelling of rectangle CFST filled with geopolymer concrete is given below. Fig 48 shows the CFST beam modelled using ANSYS. Fig 49 shows the meshed model and fig 50 shows the deformed model.

Table 5.9: Material Properties

Shape	B×D×t (mm)	L(mm)	Poisson's ratio	fy (MPa)	Es (MPa)
Square	120×120×3.84	1200	0.2	330.1	38600
Rectangle	150×120×2.93	1200	0.2	330.1	38600

The material properties of CFST with high strength concrete is given in the table 5.9. The Poisson's ratio is taken as 0.3 for steel and 0.2 for concrete . The Drucker Prager (DP) model is used for modelling the concrete. The concrete plasticity model of Drucker-Prager (DP) was employed to describe the behavior of confined concrete. The stress-strain curve of geopolymer concrete used for the analysis is given below.

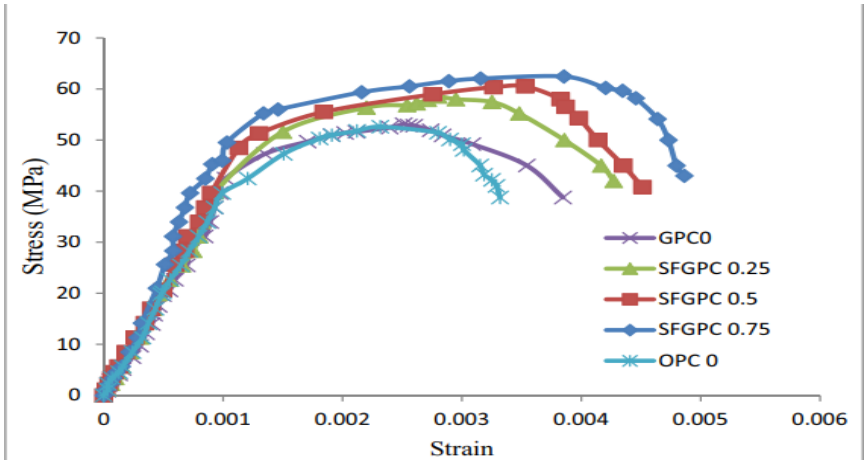

Fig 47: Stress strain graph of geopolymer concrete (Saranya et al., (2019)

The contacts between the concrete core and the steel tubes and the plates were defined as frictional with the friction coefficient of 0.5. The value of fiction coefficient was defined based on the literature review. The core concrete was model using first-order hex elements of the type SOLID 185. The CFST filled with geopolymer was modelled using the stress-strain curve obtained from Saranya et al., (2019). A surface-based interaction with a Coulomb friction model in the tangential direction and hard contact pressure model in the normal direction was used to model the interface between steel and concrete core. The friction factor in all the models was taken as 0.6. The ANSYS FE software provides various types of elements that could be used to model the steel, concrete and interface between steel and concrete.

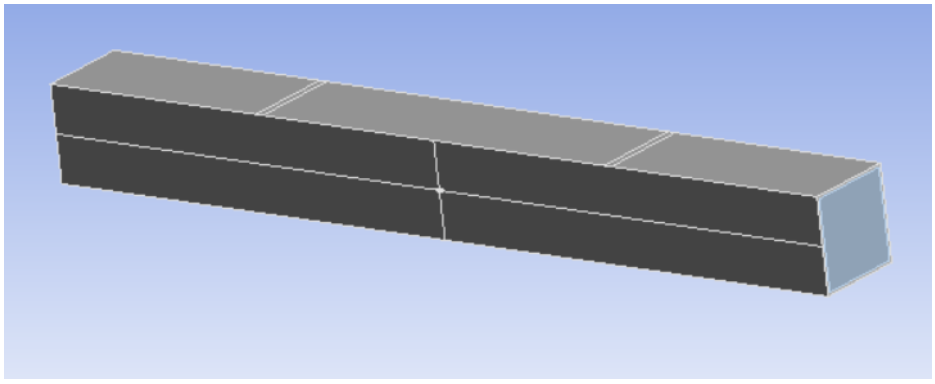

Fig 48: CFST beam modelled using ANSYS

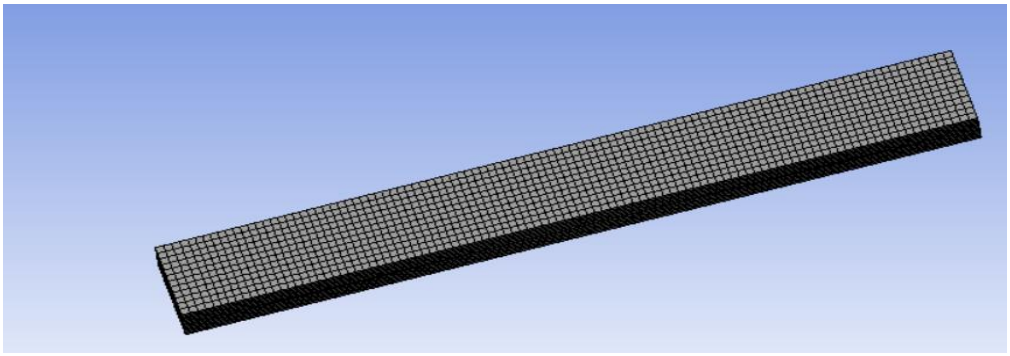

Fig 49: Meshed model

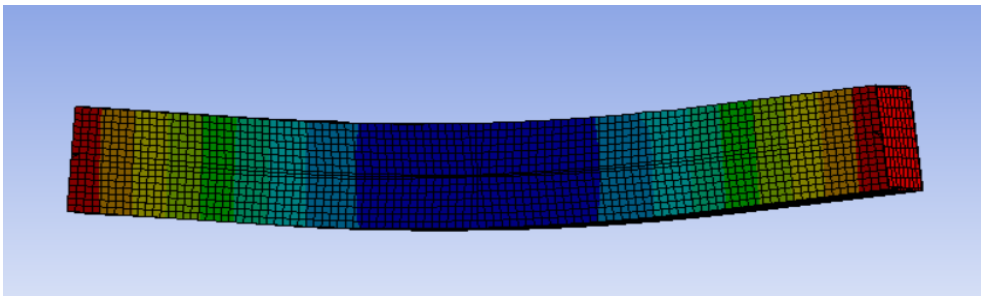

Fig 50: Deformed model

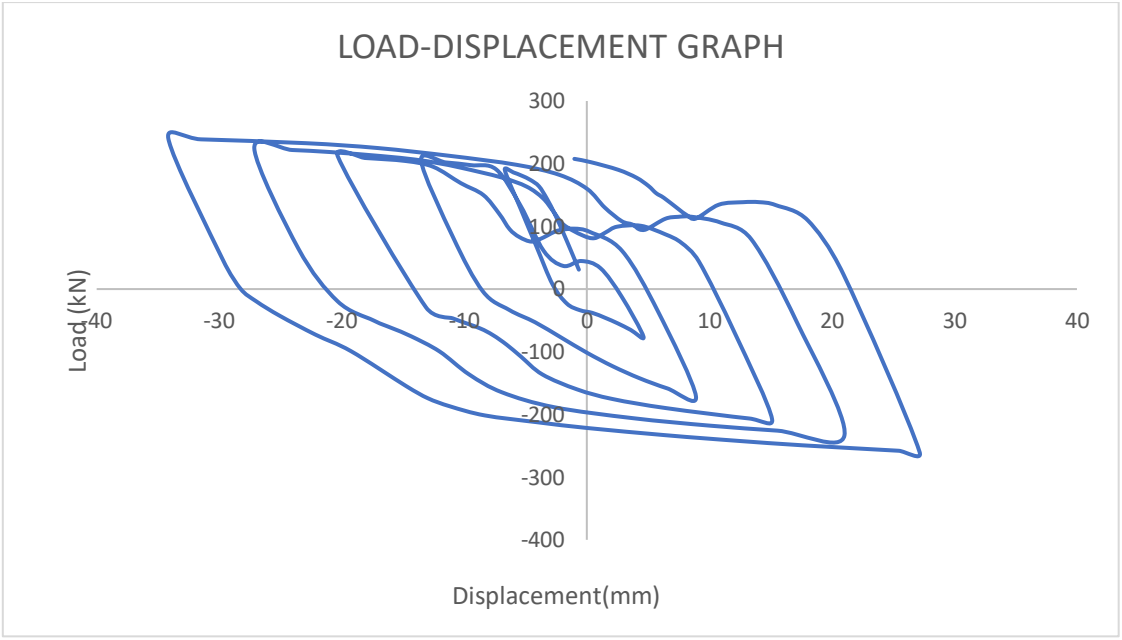

Fig 51: Load – Deflection curve

The results of the analysis the rectangle CFST filled with geopolymer concrete under cyclic loading is given in the above fig 51. The maximum load value obtained was 228.22 kN with a deflection of 30.22 mm.

5.4.4. MODELLING OF RECTANGLE CSFT FILLED WITH GEOPOLYMER CONCRETE

The modelling of rectangle CFST filled with geopolymer concrete is given below. Fig 52 shows the CFST beam modelled using ANSYS. Fig 53 shows the meshed model and fig 54 shows the deformed model.

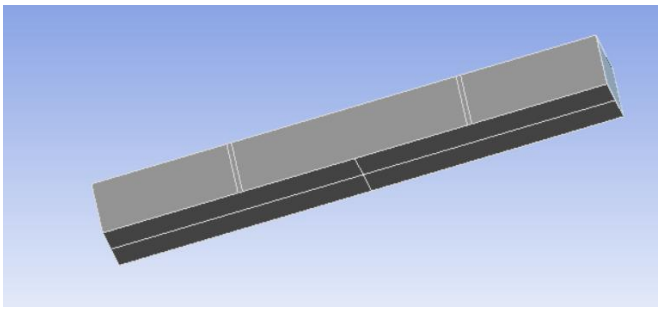

Fig 52: CFST beam modelled using ANSYS

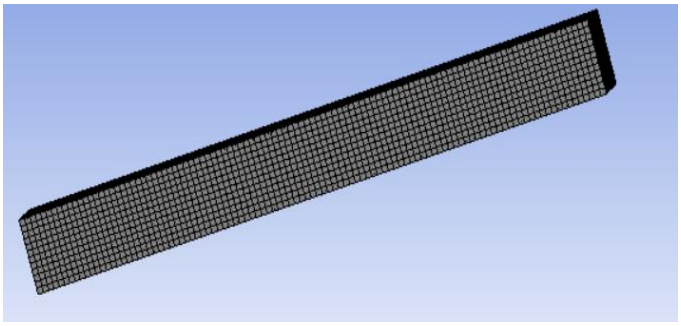

Fig 53: Meshed Model

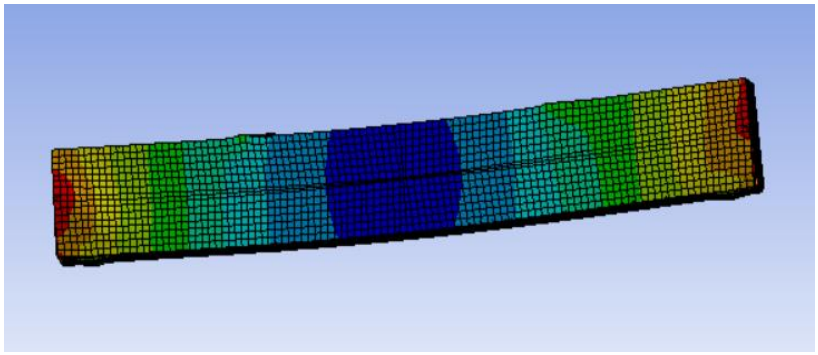

Fig 54 : Deformed model

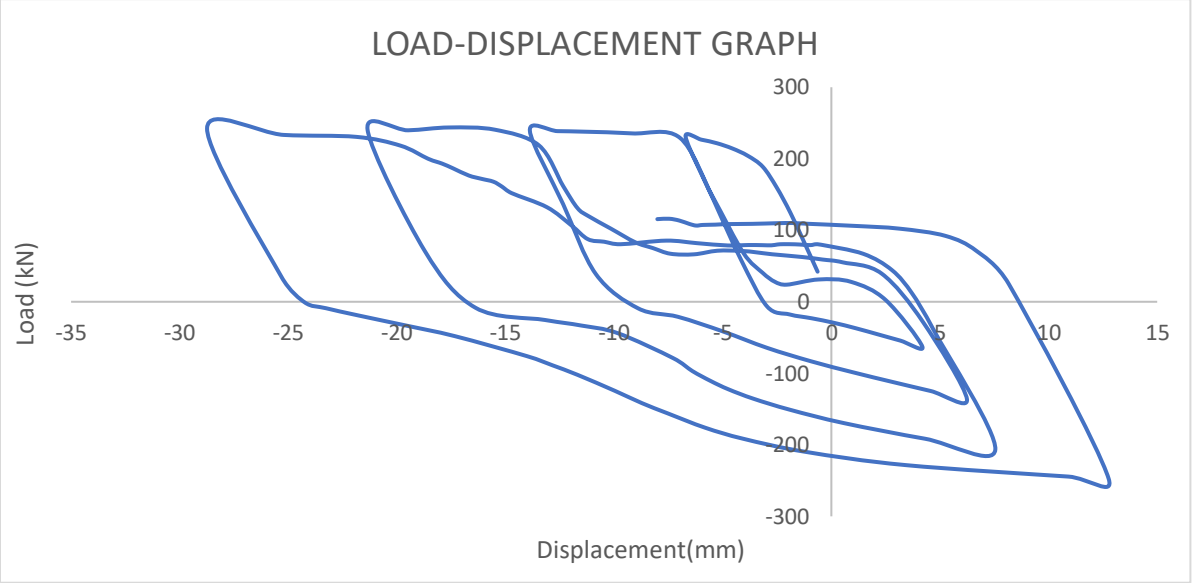

Fig 55: Load- Deflection curve

The results of the analysis the rectangle CFST filled with geopolymer under cyclic loading is given in the above fig 55. The maximum load value obtained was 242.32 kN with a deflection of 28.22 mm.

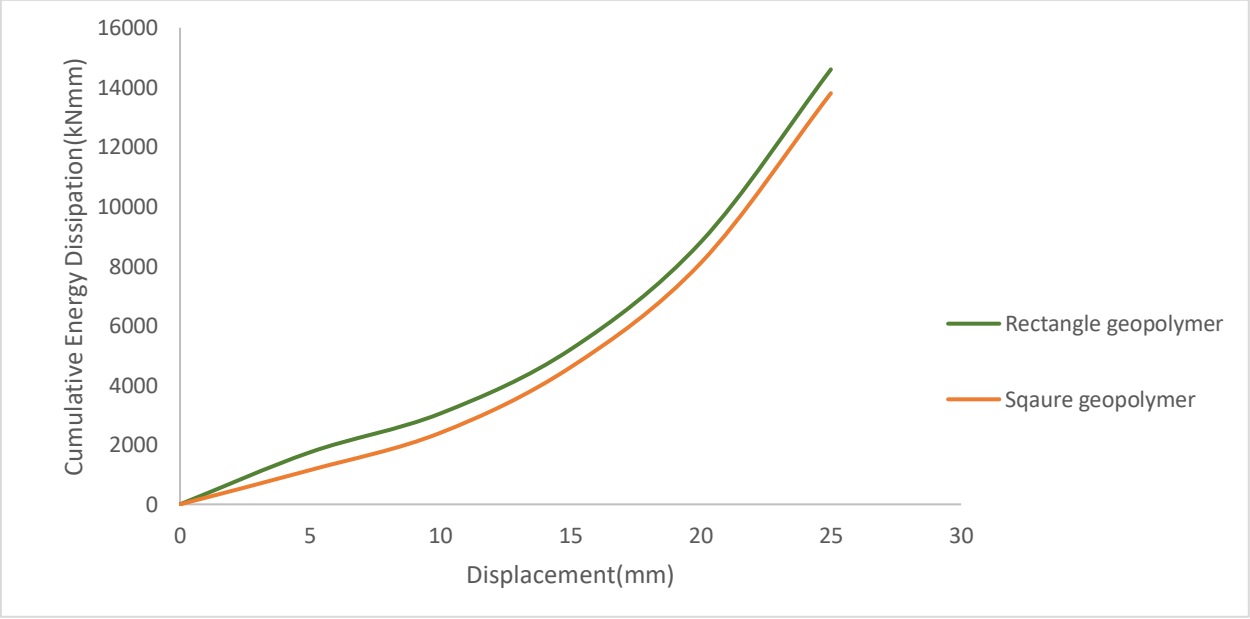

Fig 56: Cumulative energy dissipation – displacement curve

The area under the hysteresis curve for CFST filled with geopolymer concrete was found to be higher than the CFST filled with high strength concrete. It is observed that the CFST under cyclic loading was able to take more load as compared with the monotonic loading. The high strength concrete under cyclic loading was able to take 23.5% more load than the same under monotonic loading. Similarly, the geopolymer CFST under cyclic loading was able to take 6.5% more load than the same under monotonic loading.

6. PREDICTION OF FLEXURAL CAPACITY OF CFST BEAMS USING ARTIFICIAL NEURAL NETWORK (ANN)

6.1. ARTIFICIAL NEURAL NETWORK (ANN)

An artificial neural network is a technique of artificial intelligence that has the ability to learn from experiences, improving its performance by adapting to the changes in the environment. The main advantages of neural networks are the possibility of efficient manipulation of large amounts of data and its ability to generalize results. This study is aimed at demonstrating the possibilities of adapting artificial neural networks (ANN) to predict the flexural strength of CFST beams filled with high strength concrete and geopolymer concrete. Considering the great potential of this technique, this study aims to establish a comparison between Multilayer Feed forward - a Multilayer Perceptron network (MLP) with feed forward learning - and a Radial Basis Function Network (RBF). The RBF and MLP networks are usually employed in the same kind of applications (nonlinear mapping approximation and pattern recognition), however their internal calculation structures are different.

Neural networks are a series of interconnected artificial neurons which are trained by using available data to understand the underlying pattern. They consist of a series of layers with a number of processing elements within each layer. The layers can be divided into input layer, hidden layer and output layer. Information is provided to the network through the input layer, the hidden layer processes the information by applying and adjusting the weights and biases and the output layer gives the output. Each layer will have a number of processing units called neurons. The inputs are weighted to determine the amount of influence it has on the output, input signals with larger weights influence the neurons to a higher extend. An activation function is then applied to the weighted inputs, to produce an output signal by transforming the input. The input can be a single node, or it may be multiple nodes depicting different parameters where each of the input nodes acts as an input to the hidden layer. The hidden layer consists of a number of neurons/nodes which calculate the weighted sum of the input data.

The basic strategy for developing a neural-based model for material behaviour is to train a neural network on the results of a series of experiments using that material. If the experimental results contain the relevant information about the materials behaviour, then the trained neural network will contain sufficient information about the material's behaviour to qualify as a material model. Such a trained neural network not only would be able to reproduce the experimental results

it was trained on, but through its generalization capability it should be able to approximate the results of other experiments. The main benefits in using a neural network approach are that all of the behaviour of a material can be represented within the unified environment of a neural network, and the neural network-based model is built directly from experimental data using the learning capabilities of the neural network.

To train the network, the weights of connections are modified according to the information it has learned. The network learns by comparing its output for each input pattern with a target output for that pattern, then calculating the error and propagating an error function backward through the net. To run the network after it is trained, the values for the input parameters for the project are presented to the network. The network then calculates the node outputs using the existing weight values and thresholds developed in the training process. The process for running the network is extremely rapid, because the system only calculates the network node values once. To test the accuracy of a trained network, the coefficient of determination R^2 is adopted. The coefficient is a measure of how well the independent variables considered account for the measured dependent variable. The higher the R^2 value, the better the prediction relationship.

Multilayer Perceptron networks (MLP) have been applied to distinct areas, performing tasks such as function fitting and pattern recognition problems, by using the supervised training with an algorithm known as "error back propagation". A basic neuron with R inputs is shown below (Figure 1). Each input (i) is weighted with an appropriate w. The sum of the weighted inputs and the bias are forming the input to the activation function f. Eq (1) is the appropriate mathematical expression.

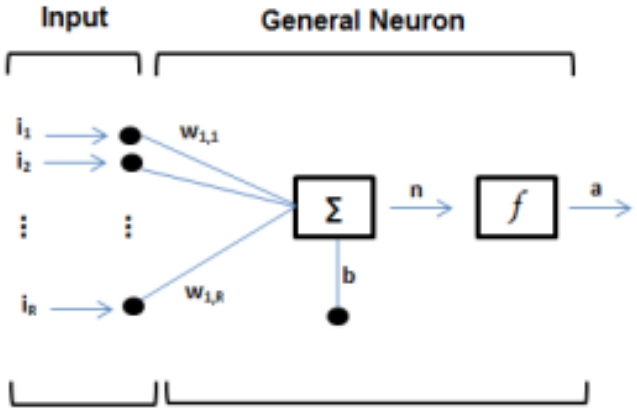

Fig 57: An elementary neuron with R inputs.

$$a = f(wi+b)$$

Where i – is the vector of input data; a – is the output signal of the neuron; w – are the weights between the neurons and b – is the bias added to the neurons. Each neuron in the network includes an activation function (f). Multilayer Perceptron networks (MLP) often have one or more hidden layers of sigmoid neurons, followed by an output layer of linear neurons. The logarithmic and hyperbolic tangent functions are the most important nonlinear activation functions for MLP. These sigmoid output neurons are often used for pattern recognition problems, while linear output neurons are used for mapping problems. Multiple layers of neurons with nonlinear activation function allow the network to learn nonlinear relationships between input and output vectors.

Radial basis function (RBF) networks have the advantages of an easy design (just three-layer architecture), good generalization, and high tolerance of input noises and ability of online learning. From the point of generalization, RBF networks can respond well to patterns that were not used for. A radial basis function neural network has an input, hidden and output layer. The input layer is composed of an input vector i. The hidden layer consists of RBF activation function as networks neuron.

The net input to the RBF activation function is the vector distance between its weight (w) and the input vector (i), multiplied by the bias b. Radial functions are a special class of functions whose value increases or decreases in relation to the distance from a central point. There are different types of radial basis functions, but the most used is the Gaussian function. RBF networks are simpler than MLP networks. In spite of having more complex architectures, it is well known that the MLP networks have been applied successfully in several difficult problems. RBFs act as local approximation networks, and their outputs are determined by specified hidden units in certain local receptive fields. On the other hand, MLP networks work globally, and the network outputs are decided by all the neurons.

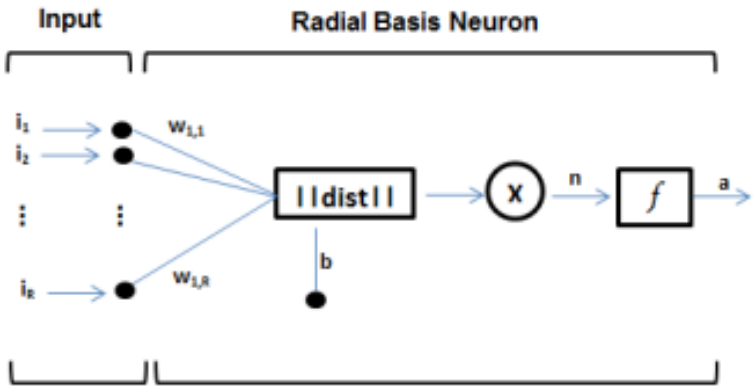

Fig 58: Radial basis network with R inputs.

$$a = radbas\ (||w-||b)$$

6.2. DATASET

The data set is collected from various literatures as well from the current study. The input variables are B(mm), H(mm), t(mm), L(mm), f_y(MPa), fc(MPa), Es(GPa),Ec(GPa) .The output variable is the flexural moment**.**

6.3. NETWORK PARAMETERS – RBF

The input layer consists of B(mm), H(mm), t(mm), L(mm), f_y (MPa), fc(MPa), Es(GPa), Ec(GPa) . The number of hidden layers chosen was 1. The number of units in hidden layer 1 was 2.The dependent variable which is the output is the flexural strength. The activation function chosen is hyperbolic tangent for the hidden layer. An activation function in a neural network defines how the weighted sum of the input is transformed into an output from a node or nodes in a layer of the network. Sometimes the activation function is called a transfer function. If the output range of the activation function is limited, then it may be called a squashing function. Many activation functions are nonlinear and may be referred to as the nonlinearity in the layer or the network design.

Network Information

Input Layer	Factors	1	fc(Mpa)
		2	fy(Mpa)
		3	L(mm)
		4	t(mm)
		5	H(mm)
		6	B(mm)
	Covariates	1	Ec(Gpa)
		2	Es(Gpa)
	Number of Units[a]		213
	Rescaling Method for Covariates		Standardized
Hidden Layer(s)	Number of Hidden Layers		1
	Number of Units in Hidden Layer 1[a]		2
	Activation Function		Hyperbolic tangent
Output Layer	Dependent Variables	1	Mu(kNm)
	Number of Units		1
	Rescaling Method for Scale Dependents		Standardized
	Activation Function		Identity
	Error Function		Sum of Squares

Fig 59: Network information

The choice of activation function has a large impact on the capability and performance of the neural network, and different activation functions may be used in different parts of the model. Technically, the activation function is used within or after the internal processing of each node in the network, although networks are designed to use the same activation function for all nodes in a layer. A network may have three types of layers: input layers that take raw input from the domain, hidden layers that take input from another layer and pass output to another layer, and output layers that make a prediction.

Out of the total 249 samples,223 were used for training and 18 were used for testing. Among them, 241 were found to be valid after excluding 8 samples. From the dataset,92.5% were used for training and the rest was used for testing. The model radial basis function was used first followed by the multilayer perceptron in neural networks.

Case Processing Summary

		N	Percent
Sample	Training	223	92.5%
	Testing	18	7.5%
Valid		241	100.0%
Excluded		8	
Total		249	

Fig 60: Case processing summary

Model Summary

Training	Sum of Squares Error	1.146
	Relative Error	.010
	Stopping Rule Used	1 consecutive step(s) with no decrease in error[a]
	Training Time	0:00:00.06
Testing	Sum of Squares Error	.250
	Relative Error	.018

Dependent Variable: Mu(kNm)

Fig 61: Model summary

The RBF procedure fits a radial basis function neural network, which is a feed forward, supervised learning network with an input layer, a hidden layer called the radial basis function layer, and an output layer. The hidden layer transforms the input vectors into radial basis functions. Like the MLP procedure, the RBF procedure performs prediction and classification. The RBF procedure trains the network in two stages:

1. The procedure determines the radial basis functions using clustering methods. The centre and width of each radial basis function are determined.

2. The procedure estimates the synaptic weights given the radial basis functions. The sum-of-squares error function with identity activation function for the output layer is used for both prediction and classification. Ordinary Least Squares regression is used to minimize the sum-of-squares error.

The input variables are B(mm), H(mm), t(mm), L(mm), fy(MPa), fc(MPa), Es(GPa),Ec(GPa) . The covariates selected was Es (GPa), Ec(GPa). The rescaling method for covariates is standardized. Activation function for the hidden layer is chosen as hyperbolic tangent. Activation function chosen for the output layer is identity. The network information is given in figure 59. The

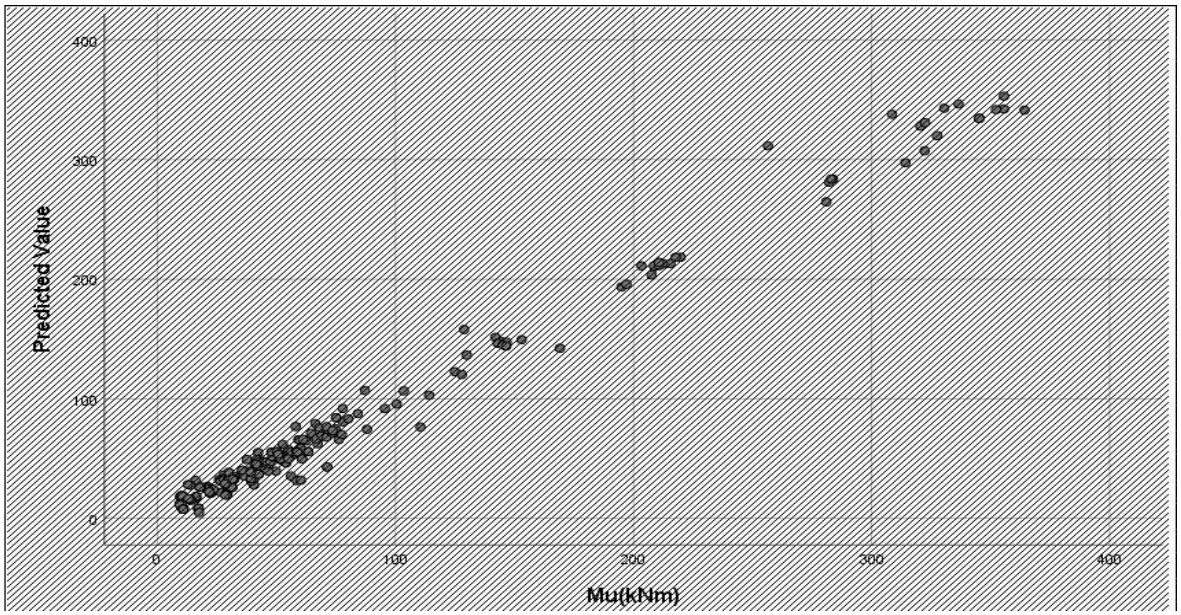

Fig 62: Graph showing predicted value against strength value using RBF

The fig (62) shows the graph of the predicted values against the original strength values obtained in lab. The network was trained in such a way that the testing set performs with good correlation between experimental and predicted data. The independent variable importance is shown in the table (3), where it shows 100% importance to yield strength of steel.

Independent Variable Importance

	Importance	Normalized Importance
fc(Mpa)	.112	53.8%
fy(Mpa)	.209	100.0%
L(mm)	.097	46.6%
t(mm)	.147	70.1%
H(mm)	.129	61.8%
B(mm)	.148	70.7%
Ec(Gpa)	.052	24.8%
Es(Gpa)	.106	50.7%

Fig 63: Independent variable importance

Table 6.1: Predicted values using RBF

S.No.	Target strength (MPa)	Output by ANN model (MPa)	Absolute error (MPa)	Relative error (%)
1.	17.2	18.16	0.96	5.58
2	12.4	11.85	0.55	4.43
3.	19.2	20.05	0.85	4.42
4.	14.2	13.76	0.44	3.09
5.	20.4	21.39	0.99	4.85
6.	23.5	22.92	0.58	2.46
7.	24.3	25.07	0.77	3.16
8	26.3	26.77	0.47	1.78
9.	26.5	25.62	0.88	3.33
10.	28.5	29.05	0.55	1.92

Table 6.1 presents the test results of the prediction of compressive strength. Relative errors and absolute errors were calculated from the modelling. The magnitude of the difference between the target output and the output through NN is the absolute error of the testing results. The dependent error is the absolute error divided by the target output. The results of the modelling were reasonably good, with minimal absolute and relative errors.

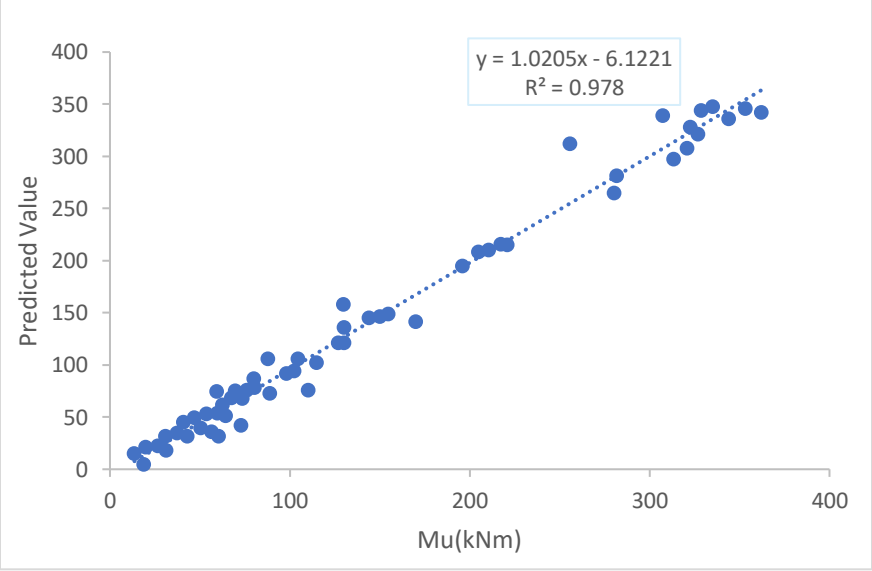

Fig 63: Graph showing predicted value against strength value

6.4. NETWORK PARAMETERS – MLP

The input layer includes B(mm), H(mm), t(mm), L(mm), f_y (MPa), fc (MPa). The covariate selected was Es (GPa), Ec(GPa) .The rescaling method for covariates is standardized. Activation function for the hidden layer is chosen as exponential. Activation function chosen for the output layer is identity. The dependent variable which is the output is the flexural strength. An activation function in a neural network defines how the weighted sum of the input is transformed into an output from a node or nodes in a layer of the network. Sometimes the activation function is called a transfer function. If the output range of the activation function is limited, then it may be called a squashing function. Many activation functions are nonlinear and may be referred to as the nonlinearity in the layer or the network design.

Network Information

Input Layer	Factors	1	fc(Mpa)
		2	fy(Mpa)
		3	L(mm)
		4	t(mm)
		5	H(mm)
		6	B(mm)
	Covariates	1	Es(Gpa)
		2	Ec(Gpa)
	Number of Units		207
	Rescaling Method for Covariates		Standardized
Hidden Layer	Number of Units[b]		173[a]
	Activation Function		Exponential
Output Layer	Dependent Variables	1	Mu(kNm)
	Number of Units		1
	Rescaling Method for Scale Dependents		Standardized
	Activation Function		Identity
	Error Function		Sum of Squares

Fig 64: Network information

The choice of activation function has a large impact on the capability and performance of the neural network, and different activation functions may be used in different parts of the model. Technically, the activation function is used within or after the internal processing of each node in the network, although networks are designed to use the same activation function for all nodes in a layer. A network may have three types of layers: input layers that take raw input from the domain, hidden layers that take input from another layer and pass output to another layer, and output layers that make a prediction.

6.4.1. RESULTS AND ANALYSIS

Out of the total 249 samples,222 were used for training and 20 were used for testing. Among them, 242 were found to be valid after excluding 7 samples. From the dataset,91.7% were used for training and the rest was used for testing. The model radial basis function was used first followed by the multilayer perceptron in neural networks. The model summary and case processing summary is given in the fig 65 and fig 66 respectively.

Model Summary

Training	Sum of Squares Error	.050
	Relative Error	.000
	Training Time	0:00:16.36
Testing	Sum of Squares Error	.299[a]
	Relative Error	.224

Fig 65: Model summary

Case Processing Summary

		N	Percent
Sample	Training	222	91.7%
	Testing	20	8.3%
Valid		242	100.0%
Excluded		7	
Total		249	

Fig 66: Case processing summary

The MLP procedure fits a particular kind of neural network called a multilayer perceptron. The multilayer perceptron is a supervised method using feed forward architecture. It can have multiple hidden layers. One or more dependent variables may be specified, which may be scale, categorical, or a combination. If a dependent variable has scale measurement level, then the neural network predicts continuous values that approximate the “true” value of some continuous function of the input data. If a dependent variable is categorical, then the neural network is used to classify

cases into the “best” category based on the input predictors. During training, the relative error obtained was 0.00 and during testing it was 0.224 which is given in the figure 65.

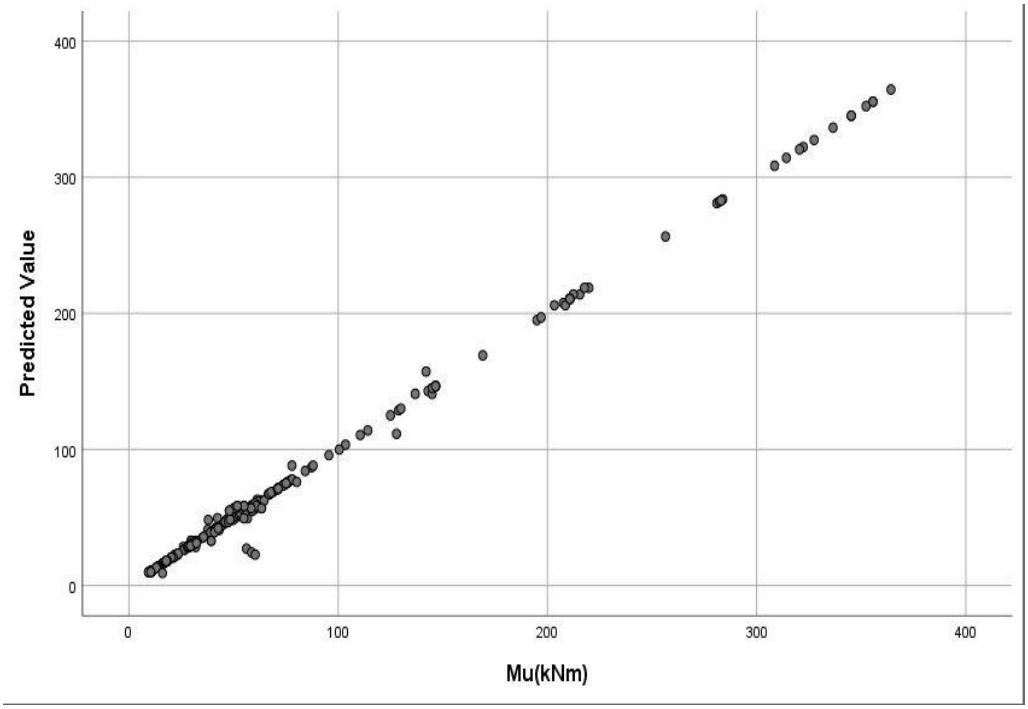

Fig 67: Graph showing predicted value against strength value using RBF

Independent Variable Importance

	Importance	Normalized Importance
fc(Mpa)	.105	46.7%
fy(Mpa)	.141	63.1%
L(mm)	.091	40.6%
t(mm)	.224	100.0%
H(mm)	.157	70.1%
B(mm)	.122	54.3%
Es(Gpa)	.107	47.7%
Ec(Gpa)	.054	23.9%

Fig 68: Independent variable importance

The fig (67) shows the graph of the predicted values against the original strength values obtained in lab. The network was trained in such a way that the testing set performs with good correlation between experimental and predicted data. The independent variable importance is shown in the table (68), where it shows 100% importance to thickness of steel.

Table 6.2: Predicted values using MLP

S.No.	Target strength (MPa)	Output by ANN model (MPa)	Absolute error (MPa)	Relative error (%)
1.	17.2	17.45	0.25	1.45
2.	12.4	12.81	0.41	3.30
3.	19.2	19.75	0.35	2.86
4.	14.2	13.82	0.38	2.67
5.	20.4	19.92	0.48	2.35
6.	23.5	24.05	0.55	2.34
7.	24.3	24.85	0.55	2.26
8.	26.3	25.95	0.35	1.33
9.	26.5	27.27	0.77	2.90
10.	28.5	28.94	0.44	1.54

Table 6.2 presents the test results of the prediction of compressive strength. Relative errors and absolute errors were calculated from the modelling. The magnitude of the difference between the target output and the output through NN is the absolute error of the testing results. The dependent error is the absolute error divided by the target output. The results of the modelling were reasonably good, with minimal absolute and relative errors.

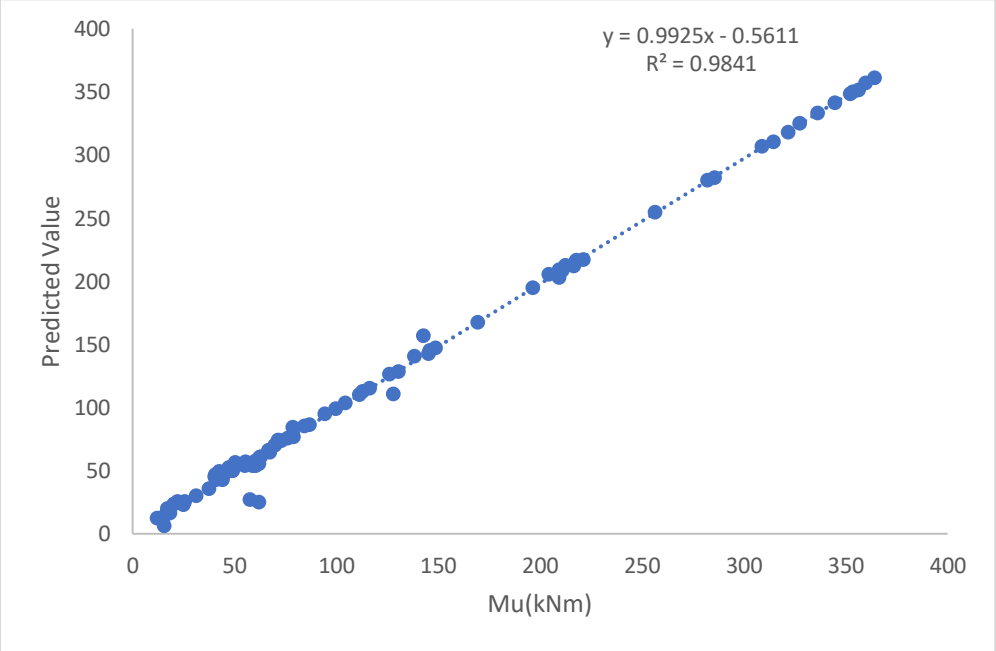

Fig 69: Graph showing predicted value against strength value

6.5. RESULTS AND DISCUSSION

From the results, it was observed that the two types of networks (Multilayer Perceptron and Radial Basis Function) were able to predict the results satisfactorily. However, the Multilayer Perceptron network showed higher accuracy than the radial basis function. The R^2 value of MLP analysis was found to be better than RBF. The MLP networks showed smaller maximum absolute errors than models developed using RBF. The technological advancements in the field of machine learning pave a great way to reach interdisciplinary research application. One such problem in civil engineering, to find a mathematical relationship for the amount of different components used for creating a concrete mix and the compression strength was considered. From the results, it was observed that the two types of networks (Multilayer Perceptron and Radial Basis Function) were able to predict the results satisfactorily. However, the Multilayer Perceptron network showed higher accuracy than the radial basis function. The R^2 value of MLP analysis was found to be better than RBF. The MLP networks showed smaller maximum absolute errors than models developed using RBF.

7. RESULTS AND CONCLUSION

In this study, numerical investigations were carried out to study the flexural behavior of square and rectangular CFST members. The load-deformation curves and ultimate moment capacity obtained numerically was found to be in good agreement with experimental results in the validation step. The FE model was used to investigate the effect of different parameters on the flexural performance of square and rectangular CFST beams. Two different concrete infills – high strength concrete and geopolymer concrete was used to analyze the behavior. The numerical investigation is done using ANSYS software.

The Drucker Prager (DP) model was used for modelling the concrete. The concrete plasticity model of Drucker-Prager (DP) was employed to describe the behavior of confined concrete. An extensive parametric study was performed to investigate the influences of depth-to-thickness ratio (28.57−200), effect of D/B ratio (24- 42.8) and steel yield strengths (235-420 MPa) on the fundamental behavior of CFST beams under flexure load.The comparison on a rectangular type of CFST and a square CFST is also done based on these factors.

When the D/B ratio increased from 0.54 to 2, the ultimate capacity of members is increased by more than 50%. In the analysis, the geopolymer filled CFST was able to take more load as compared with the high strength concrete. It can be seen that by increasing D/t ratio from 28.57 to 200 (7 times), the ultimate bending moment capacity reduced from 207.8 to 21 kN-m (almost 8 times) for square CFST beams. The reduction in ultimate bending moment capacity is attributed to the fact that the beam having larger D/t ratio has a lesser area of steel. The ultimate flexure strength of square CFST beams was found to increase significantly with an increase in the yield strength of steel. By increasing the yield strength of steel from 235 MPa to 420 MPa, the ultimate flexure load of the square CFST beam was found to increase. The concrete-filled steel tubular (CFST) structure offers numerous structural benefits, including high strength and fire resistances, favourable ductility and large energy absorption capacities. There is also no need for the use of shuttering during concrete construction; hence, the construction cost and time are reduced. These advantages have been widely exploited and have led to the extensive use of concrete filled tubular structures in civil engineering structures.

Also, an artificial neural network prediction model was developed to predict the flexural strength of the CFST models . This study is aimed at demonstrating the possibilities of adapting artificial neural networks (ANN) to predict the compressive strength of high-performance concrete. Considering the great potential of this technique, this study aims to establish a comparison between Multilayer Feed forward - a Multilayer Perceptron network (MLP) with feed forward learning - and a Radial Basis Function Network (RBF). The RBF and MLP networks are usually employed in the same kind of applications (nonlinear mapping approximation and pattern recognition), however their internal calculation structures are different. From the results, it was observed that the two types of networks (Multilayer Perceptron and Radial Basis Function) were able to predict the results satisfactorily. However, the Multilayer Perceptron network showed higher accuracy than the radial basis function. The R^2 value of MLP analysis was found to be better than RBF. The MLP networks showed smaller maximum absolute errors than models developed using RBF.

8.REFERENCES

- Ellobody, E..,Young,B., Lam,D., (2016),"Behaviour of Normal and High Strength Concrete-Filled Compact Steel Tube Circular Stub Columns", *Journal of Construction Steel Research,* Volume 62, Issue 7, Pages 706-715.
- Evirgen,H., Tuncan,A.,(2014) ,"Structural behaviour of concrete filled steel tubular sections (CFT/CFSt) under axial compression" , *Thin-Walled Structures, Elsevier,* Volume 80, Pages 46-56
- Hana.L.,H., Maa,D.,Y.,Zhou,H., 12th International Conference on Advances in Steel-Concrete Composite Structures (ASCCS 2018)
- Han, L., H.,Li.W, Bjorhovde,R (2018), "Developments and advanced applications of concrete-filled steel tubular (CFST) structures: Members", *Journal of constructional steel research, Elsevier,* Volume 100, Pages 211-228
- Han,L.,H.,Song,T.,Y., Tan,Q.,H.,(2012),"Fire performance of steel-concrete composite structures in China: test, analysis and design approach", Proceedings Of The 10Th International Conference On Advances In Steel Concrete Composite And Hybrid Structures, Singapore
- Jayashri,M.,,Helena,H.,J., (2021), "Behaviour of Concrete-Filled Steel Tubular Columns: A State of the Art Review", *International Research Journal of Engineering and Technology (IRJET*),Volume: 08 ,Issue: 08
- Soudararajan, A., Shanmughasundaram,K.,(2008)," Flexural behaviour of concrete-filled steel hollow sections beams", *Journal of Civil Engineering and Management* ,Volume 14, 2008 ,Issue 2.
- Hua, W., Wang, H.,Hasegawa,A.,(2014), "Experimental study on reinforced concrete filled circular steel tubular columns" , *An International Journal on Steel and Composite Structures,*Vol.17, No.4.
- L.-H. Han, W. Li, R. Bjorhovde, (2014), "Developments and advanced applications of concrete-filled steel tubular (CFST) structures", *Journal of Construction Steel Research*, Volume 100, September 2014, Pages 211-228.
- Han,L.,H.,(2014)," Flexural behaviour of concrete-filled steel tubes", *Journal of Constructional Steel Research* ,Issue :60 , pg 313–337.

- T. Yu, Y.M. Hu, J.G. Teng, (2016), Cyclic lateral response of FRP-confined circular concrete filled steel tubular columns, *Journal of Construction Steel Research*,124,12–22.
- Y.-F. Yang, (2015), "Modelling of recycled aggregate concrete-filled steel tube (RACFST) beam-columns subjected to cyclic loading", *Steel Composite Structures*, Issue:18, pg 213–233.
- A. Silva, Y. Jiang, J. Castro, N. Silvestre, (2016)," Experimental assessment of the flexural behavior of circular rubberized concrete-filled steel tubes*", Journal of Construction Steel Research,* Issue :122,pages: 557–570.
- G. Li, D. Liu, Z. Yang, C. Zhang, (2017)," Flexural behavior of high strength concrete filled high strength square steel tube", *Journal of Construction Steel Research,* Volume:128, pages:732–744.
- W.-H. Wang, L.-H. Han, W. Li, Y.-H. Jia, (2014)," Behavior of concrete-filled steel tubular stub columns and beams using dune sand as part of fine aggregate", *Construction Building Materials*, volume: 51, pages :352–363.
- S. Guler, A. Copur, M. Aydogan, (2012)," Flexural behaviour of square UHPC-filled hollow steel section beams", *Structural Engineering Mechanics*, Volume: 43 ,pages:225–237.
- M. Sundararaja, G.G. Prabhu, (2011), "Finite element modelling of CFRP jacketed CFST members under flexural loading", *Thin-Walled Structures*, Volume: 49 , Pages: 1483–1491.
- M. Elchalakani, A. Karrech, M. Hassanein, B. Yang, (2016)," Plastic and yield slenderness limits for circular concrete filled tubes subjected to static pure bending", *Thin-Walled Structures*, Volume :109, pages:50–64.
- P Saranya, P Nagarajan, AP Shashikala, (2019), "Performance evaluation of geopolymer concrete beams under monotonic loading", *Structures*, Volume 20, August 2019, Pages 560-569.
- Han, L.; Ma, D.; Zhou, K. (2018), "Concrete-encased CFST structures: behaviour and application", En Proceedings of the 12th International Conference on Advances in Steel-Concrete Composite Structures. ASCCS 2018.
- A.Farid, A . Yosri ,A. Yazan,(2021), Effect of different cross-sections and concrete types on the flexural behavior of CFSTs, *Composite Structures*, Volume 276, November 2021.

- Q. Qing, (2011), High strength circular concrete-filled steel tubular slender beam–columns, Part I: Numerical analysis, *Journal of Constructional Steel Research, Volume* 67, Issue 2, February 2011, Pages 164-171.
- Q. Qing, (2011), High strength circular concrete-filled steel tubular slender beam–columns, Part II: Fundamental Behaviour, *Journal of Constructional Steel Research, Volume* 67, Issue 2, February 2011, Pages 164-171.
- J. M. Flor, R ,H. Fakury ,R. B. Caldas , F. C. Rodrigues ,A. H. M. Araújo, "Experimental study on the flexural behaviour of large-scale rectangular concrete-filled steel tubular beams",*Ibracon,*Volume 10,August 2017.
- Omar, J. Butterworth, P. Lowe,(2000), "Development of finite element model for concrete-filled steel tube members in flexure", Proceedings of the 7th New Zealand Postgraduate Conference on Engineering and Technology, Palmerston North.
- Tao, Z., Wang, Z.B., Yu, Q. (2013).,"Finite element modelling of concrete-filled steel stub columns under axial compression" ,Journal of Construction Steel Research, Issue 89, pages 121-131.
- H. Fang, P. Visintin, (2022), "Structural performance of geopolymer-concrete-filled steel tube members subjected to compression and bending", *Journal of Constructional Steel Research*, Volume 188, January 2022.
- M Sifan, P Gatheeshgar, S Navaratnam,(2022), "Flexural behaviour and design of hollow flange cold-formed steel beam filled with lightweight normal and lightweight high strength concrete", *Journal of building engineering*, Volume 48, 1 May 2022.
- F.Gaoab,H.P.Zhuab,D.H.Zhangab,T.S.Fangab,(2014),"Experimental investigation on flexural behaviour of concrete-filled pentagonal flange beam under concentrated loading", Volume 84, November 2014, Pages 214-225.

APPENDIX

S.NO.	B(mm)	H(mm)	t(mm)	L(mm)	fy(Mpa)	fc(Mpa)	Es(Gpa)	Ec(Gpa)	Mu(kNm)	Reference
1	150	250	5	3000	350	60	200	36.6	142	Ruin wang et al
2	250	250	5	3000	350	60	200	36.6	195	Ruin wang et al
3	125	250	5	3000	350	60	200	36.6	125	Ruin wang et al
4	150	250	12.5	3000	350	60	200	36.6	281	Ruin wang et al
5	150	250	2.5	3000	350	60	200	36.6	76	Ruin wang et al
6	100	150	3.7	2000	444	36.8	200	28.5	49.1	Ahmed et al
7	100	150	3.7	2000	444	36.8	200	28.5	51.7	Ahmed et al
8	100	150	3.47	2000	444	36.8	200	28.5	50.9	Ahmed et al
9	75	125	2.8	2000	445	31.5	200	28.5	29.7	Al Zand et al
10	75	125	2.8	2000	445	31.5	200	28.5	30.8	Al Zand et al
11	75	125	2.8	2000	445	31.5	200	28.5	39.3	Al Zand et al
12	75	125	2.8	2000	445	31.5	200	28.5	32	Al Zand et al
13	75	125	2.8	2000	445	31.5	200	28.5	29.7	Al Zand et al
14	140	140	5	2000	300	22.3	200	22.1	48	Wang et al
15	140	140	5	2000	300	22.3	200	22.1	56.2	Wang et al
16	140	140	5	2000	300	22.3	200	22.1	58.8	Wang et al
17	140	140	5	2000	300	26.4	200	24.14	50.8	Wang et al
18	140	140	5	2000	300	26.4	200	24.14	52.6	Wang et al
19	140	140	5	2000	300	26.4	200	24.14	60.2	Wang et al
20	140	140	5	2000	300	32.8	200	26.9	51.8	Wang et al
21	140	140	5	2000	300	32.8	200	26.9	55	Wang et al
22	140	140	5	2000	300	32.8	200	26.9	60.8	Wang et al
23	140	140	5	2000	300	40	200	29.7	50.2	Wang et al
24	140	140	5	2000	300	40	200	29.7	58.4	Wang et al
25	140	140	5	2000	300	40	200	29.7	63.4	Wang et al
26	120	120	3.84	1100	330.1	27.3	200	24.5	29.34	Muhammed et al
27	120	120	3.84	1100	330.1	35.2	200	27.8	30.16	Muhammed et al
28	120	120	3.84	1100	330.1	35.2	200	27.8	32.25	Muhammed et al
29	120	120	3.84	1100	330.1	35.2	200	27.8	31.69	Muhammed et al
30	120	120	5.86	1100	321.1	31.3	200	26.2	40.9	Muhammed et al
31	120	120	5.86	1100	321.1	31.3	200	26.2	41.54	Muhammed et al
32	120	120	5.86	1100	321.1	40	200	29.7	41.43	Muhammed et al
33	120	120	5.86	1100	321.1	40	200	29.7	42.61	Muhammed et al
34	150	120	2.93	1100	293.8	34.5	200	27.6	31.4	Muhammed et al
35	150	120	2.93	1100	293.8	34.5	200	27.6	31.4	Muhammed et al
36	120	90	2.93	1100	293.8	34.5	200	27.6	21.1	Muhammed et al
37	120	90	2.93	1100	293.8	34.5	200	27.6	20.2	Muhammed et al
38	150	90	2.93	1100	293.8	34.5	200	27.6	28.4	Muhammed et al
39	150	90	2.93	1100	293.8	34.5	200	27.6	29.4	Muhammed et al
40	120	60	2.93	1100	293.8	34.5	200	27.6	18.4	Muhammed et al

41	120	60	2.93	1100	293.8	34.5	200	27.6	17.8	Muhammed et al
42	152	152	4.8	1975	389	47	200	32.22	73.6	Muhammed et al
43	152	152	4.8	2430	389	42.08	200	30.7	75.1	Muhammed et al
44	152	152	4.8	3040	389	41.2	200	30.16	71.3	Muhammed et al
45	152	152	9.5	1976	432	46.9	200	32.18	146.5	Muhammed et al
46	254	152	6.4	2231	377	46.7	200	32.66	210.7	Muhammed et al
47	254	152	6.4	3243	377	45.2	200	31.5	210.7	Muhammed et al
48	254	152	6.4	4260	377	44.3	200	31.28	207.6	Muhammed et al
49	254	152	9.5	2231	394	46.2	200	32.11	283.8	Muhammed et al
50	254	152	9.5	4260	394	43.8	200	31.11	282.2	Muhammed et al
51	152	254	6.4	1970	377	47.1	200	32.22	144.7	Muhammed et al
52	152	254	6.4	2432	377	42.1	200	30.55	146.7	Muhammed et al
53	152	254	6.4	3041	377	40.5	200	29.99	142.9	Muhammed et al
54	126	126	3	1800	300	50	200	33.22	27.9	Muhammed et al
55	156	156	3	2250	300	50	200	33.22	42.4	Muhammed et al
56	186	186	3	2700	300	32	200	36.58	62.6	Muhammed et al
57	246	246	3	3600	300	38	200	28.97	103.5	Muhammed et al
58	306	306	3	4500	300	22	200	28.97	153	Muhammed et al
59	305	405	9.5	1200	345	32.6	210	26.8	734.85	Muhammed et al
60	72	72	3.2	1200	345	32.6	210	26.8	10.06	Muhammed et al
61	72	72	3.2	1200	345	32.6	210	26.8	9.57	Muhammed et al
62	72	72	3.2	1200	345	32.5	210	26.8	10.4	Muhammed et al
63	72	72	3.2	1200	345	32.5	210	26.8	9.9	Muhammed et al
64	72	72	3.2	1200	345	32.5	210	26.8	10.07	Muhammed et al
65	72	72	3.2	1200	345	21.63	210	21.8	10.4	Muhammed et al
66	72	72	3.2	1200	345	21.63	210	21.8	9.74	Muhammed et al
67	72	72	3.2	1200	345	21.63	210	21.8	10	Muhammed et al
68	72	72	3.2	1200	345	21.63	210	21.8	10.23	Muhammed et al
69	100	100	1.9	1400	282	81.3	201.5	42.3	10.83	Muhammed et al
70	100	100	1.9	1400	282	81.3	201.5	42.3	9.96	Muhammed et al
71	100	100	1.9	1400	282	81.3	201.5	42.3	10.33	Muhammed et al
72	200	200	1.9	1400	282	81.3	201.5	42.3	42.3	Muhammed et al
73	200	200	1.9	1400	282	81.3	201.5	42.3	54.94	Muhammed et al
74	200	200	1.9	1400	282	81.3	201.5	42.3	56.7	Muhammed et al
75	140	140	3	840	235	62.6	200.1	37.1	31.9	Muhammed et al
76	140	140	3	840	235	62.6	200.1	37.1	27.5	Muhammed et al
77	140	140	3	1680	235	62.6	200.1	37.1	29.4	Muhammed et al
78	140	140	3	840	235	62.6	200.1	37.1	25.9	Muhammed et al
79	140	140	3	1680	235	62.6	200.1	37.1	30.2	Muhammed et al
80	140	140	3	1680	235	62.6	200.1	37.1	29.4	Muhammed et al
81	180	180	3	900	235	62.6	200.1	37.1	37.6	Muhammed et al
82	180	180	3	900	235	62.6	200.1	37.1	43.1	Muhammed et al
83	180	180	3	1800	235	62.6	200.1	37.1	37.9	Muhammed et al
84	180	180	3	900	235	62.6	200.1	37.1	41.7	Muhammed et al

85	180	180	3	1800	235	62.6	200.1	37.1	49.8	Muhammed et al
86	180	180	3	1800	235	62.6	200.1	37.1	46.5	Muhammed et al
87	80	80	2.5	1100	288	150	200	57.5	9.92	Muhammed et al
88	80	80	2.5	1100	288	150	200	57.5	10.42	Muhammed et al
89	80	80	2.5	1100	288	150	200	57.5	9.26	Muhammed et al
90	80	80	3	1100	277	150	200	57.5	10.67	Muhammed et al
91	80	80	3	1100	277	150	200	57.5	10.9	Muhammed et al
92	80	80	3	1100	277	150	200	57.5	11.21	Muhammed et al
93	80	80	4	1100	268	150	200	57.5	17.03	Muhammed et al
94	80	80	4	1100	268	150	200	57.5	17.35	Muhammed et al
95	250	150	5.9	1600	409	70.6	208	39.49	215.5	Muhammed et al
96	250	150	5.9	1600	409	70.6	208	39.49	212.4	Muhammed et al
97	250	150	5.9	1600	409	90.9	208	44.8	219.8	Muhammed et al
98	250	150	5.9	1600	409	90.9	208	44.8	217.7	Muhammed et al
99	160	160	3.46	4040	363	78	203	41.5	59.3	Muhammed et al
100	160	160	3.46	4040	363	78	203	41.5	59.5	Muhammed et al
101	160	240	3.46	4040	363	78	203	41.5	136.8	Muhammed et al
102	160	240	3.46	4040	363	78	203	41.5	144.9	Muhammed et al
103	160	320	3.46	4040	363	78	203	41.5	208.6	Muhammed et al
104	160	320	3.46	4040	363	78	203	41.5	203.3	Muhammed et al
105	150	150	2	1998	400	56	209	35.17	26.7	Muhammed et al
106	150	150	3	2002	400	56	209	35.17	40.63	Muhammed et al
107	100	200	2	2002	400	56	209	35.17	22.32	Muhammed et al
108	100	200	3	2000	400	56	209	35.17	30.27	Muhammed et al
109	100	200	5	1100	235	50	200	32.6	52.7	Muhammed et al
110	100	200	5	1100	275	50	200	32.6	61.21	Muhammed et al
111	100	200	5	1100	300	50	200	32.6	66.43	Muhammed et al
112	100	200	5	1100	355	50	200	32.6	77.88	Muhammed et al
113	100	200	5	1100	400	50	200	32.6	87.24	Muhammed et al
114	200	200	5	1100	235	50	200	32.6	75.87	Muhammed et al
115	200	200	5	1100	275	50	200	32.6	88.022	Muhammed et al
116	200	200	5	1100	300	50	200	32.6	95.562	Muhammed et al
117	200	200	5	1100	355	50	200	32.6	114.18	Muhammed et al
118	200	200	5	1100	400	50	200	32.6	127.866	Muhammed et al
119	100	200	1	1100	275	50	200	29	21	Muhammed et al
120	100	200	2	1100	275	50	200	29	39.375	Muhammed et al
121	100	200	4	1100	275	50	200	29	76.23	Muhammed et al
122	100	200	6	1100	275	50	200	29	110.5335	Muhammed et al
123	100	200	10	1100	275	50	200	29	169.1163	Muhammed et al
124	200	200	1	1100	275	50	200	29	16	Muhammed et al
125	200	200	2	1100	275	50	200	29	30	Muhammed et al
126	200	200	4	1100	275	50	200	29	58.08	Muhammed et al
127	200	200	6	1100	275	50	200	29	84.216	Muhammed et al
128	200	200	10	1100	275	50	200	29	128.8505	Muhammed et al

129	100	200	2.5	1100	275	2	200	29	28.154	Muhammed et al
130	100	200	2.5	1100	275	4	200	29	26.6	Muhammed et al
131	100	200	2.5	1100	275	8	200	29	26.387	Muhammed et al
132	100	200	2.5	1100	275	16	200	29	27.978	Muhammed et al
133	100	200	2.5	1100	275	32	200	29	31.678	Muhammed et al
134	100	200	2.5	1100	275	50	200	29	35.054	Muhammed et al
135	100	200	2.5	1100	275	60	200	29	36.57831	Muhammed et al
136	100	200	2.5	1100	275	80	200	29	39.034	Muhammed et al
137	100	200	2.5	1100	275	100	200	29	40.881	Muhammed et al
138	100	200	5	1100	275	2	200	29	67.317	Muhammed et al
139	100	200	5	1100	275	4	200	29	61.837	Muhammed et al
140	100	200	5	1100	275	8	200	29	58.186	Muhammed et al
141	100	200	5	1100	275	16	200	29	57.2979	Muhammed et al
142	100	200	5	1100	275	32	200	29	60.2313	Muhammed et al
143	100	200	5	1100	275	50	200	29	64.5253	Muhammed et al
144	100	200	5	1100	275	60	200	29	66.834	Muhammed et al
145	100	200	5	1100	275	80	200	29	69.022	Muhammed et al
146	100	200	5	1100	275	100	200	29	71.0789	Muhammed et al
147	200	120	5	1100	345	40	200	29.7	43.198	Muhammed et al
148	178	142	5	1100	345	40	200	29.7	50.534	Muhammed et al
149	160	160	5	1100	345	40	200	29.7	56.167	Muhammed et al
150	120	200	5	1100	345	40	200	29.7	67.931	Muhammed et al
151	107	214	5	1100	345	40	200	29.7	71.473	Muhammed et al
152	200	120	5	1100	345	60	200	36.4	44.8	Muhammed et al
153	178	142	5	1100	345	60	200	36.4	52.56	Muhammed et al
154	160	160	5	1100	345	60	200	36.4	58.541	Muhammed et al
155	120	200	5	1100	345	60	200	36.4	71.066	Muhammed et al
156	107	214	5	1100	345	60	200	36.4	74.81499	Muhammed et al
157	200	120	5	1100	345	80	200	42.3	46.03	Muhammed et al
158	178	142	5	1100	345	80	200	42.3	54.086	Muhammed et al
159	160	160	5	1100	345	80	200	42.3	60.323	Muhammed et al
160	120	200	5	1100	345	80	200	42.3	73.505	Muhammed et al
161	107	214	5	1100	345	80	200	42.3	77.479	Muhammed et al
162	100	100	4.54	950	392	30.65	200	26.02	29.29	Ahmed et al
163	100	100	4.54	950	392	30.65	200	26.02	28.48	Ahmed et al
164	100	100	4.54	950	392	37.21	200	28.67	29.15	Ahmed et al
165	100	100	4.54	950	392	37.21	200	28.67	29.44	Ahmed et al
166	100	100	2.71	950	315	30.65	200	26.02	16.31	Ahmed et al
167	100	100	2.71	950	315	30.65	200	26.02	15.94	Ahmed et al
168	100	100	2.71	950	315	37.21	200	28.67	16.36	Ahmed et al
169	100	100	2.71	950	315	37.21	200	28.67	16.17	Ahmed et al
170	120	120	4.69	950	343	30.65	200	26.02	46.04	Ahmed et al
171	120	120	4.69	950	343	30.65	200	26.02	47.46	Ahmed et al
172	120	120	4.69	950	343	37.21	200	28.67	48.59	Ahmed et al

173	120	120	4.69	950	343	37.21	200	28.67	48.3	Ahmed et al
174	120	120	2.8	950	261	30.65	200	26.02	23.22	Ahmed et al
175	120	120	2.8	950	261	30.65	200	26.02	21.83	Ahmed et al
176	120	120	2.8	950	261	37.21	200	28.67	23.23	Ahmed et al
177	120	120	2.8	950	261	37.21	200	28.67	23.49	Ahmed et al
178	100	100	4.54	950	392	37.21	200	28.67	18.04	Ahmed et al
179	100	100	2.71	950	315	37.21	200	28.67	7.48	Ahmed et al
180	120	120	4.69	950	343	37.21	200	28.67	24.96	Ahmed et al
181	120	120	2.8	950	261	37.21	200	28.67	8.07	Ahmed et al
182	120	120	3.84	1200	330.1	60.9	364.8	36.6	17.56	Current study
183	120	120	3.84	1200	330.1	60.9	364.8	36.6	19.06	Current study
184	120	120	3.84	1200	330.1	60.9	364.8	36.6	12.07	Current study
185	120	120	3.84	1200	330.1	60.9	364.8	36.6	14.12	Current study
186	100	200	1	1200	330.1	60.9	364.8	36.6	15.16	Current study
187	100	200	3	1200	330.1	60.9	364.8	36.6	16.15	Current study
188	100	200	5	1200	330.1	60.9	364.8	36.6	17.85	Current study
189	100	200	7	1200	330.1	60.9	364.8	36.6	18.88	Current study
190	200	200	1	1200	330.1	60.9	364.8	36.6	16.11	Current study
191	200	200	3	1200	330.1	60.9	364.8	36.6	17.85	Current study
192	200	200	5	1200	330.1	60.9	364.8	36.6	18.55	Current study
193	200	200	7	1200	330.1	60.9	364.8	36.6	19.22	Current study
194	100	200	1	1200	330.1	51.25	364.8	36.6	16.99	Current study
195	100	200	3	1200	330.1	51.25	364.8	36.6	17.25	Current study
196	100	200	5	1200	330.1	51.25	364.8	36.6	18.22	Current study
197	100	200	7	1200	330.1	51.25	364.8	36.6	18.99	Current study
198	200	200	1	1200	330.1	51.25	364.8	36.6	17.01	Current study
199	200	200	3	1200	330.1	51.25	364.8	36.6	17.56	Current study
200	200	200	5	1200	330.1	51.25	364.8	36.6	18.55	Current study
201	200	200	7	1200	330.1	51.25	364.8	36.6	18.96	Current study
202	100	200	5	1200	235	60.9	364.8	36.6	20.45	Current study
203	100	200	5	1200	345	60.9	364.8	36.6	24.32	Current study
204	100	200	5	1200	390	60.9	364.8	36.6	26.56	Current study
205	100	200	5	1200	420	60.9	364.8	36.6	28.99	Current study
206	200	200	5	1200	235	60.9	364.8	36.6	17.72	Current study
207	200	200	5	1200	345	60.9	364.8	36.6	24.51	Current study
208	200	200	5	1200	390	60.9	364.8	36.6	27.22	Current study
209	200	200	5	1200	420	60.9	364.8	36.6	29.27	Current study
210	100	200	5	1200	235	51.25	364.8	36.6	23.54	Current study
211	100	200	5	1200	345	51.25	364.8	36.6	26.34	Current study
212	100	200	5	1200	390	51.25	364.8	36.6	28.65	Current study
213	100	200	5	1200	420	51.25	364.8	36.6	30.51	Current study
214	200	200	5	1200	235	51.25	364.8	36.6	19.81	Current study
215	200	200	5	1200	345	51.25	364.8	36.6	26.41	Current study
216	200	200	5	1200	390	51.25	364.8	36.6	28.84	Current study

217	200	200	5	1200	420	51.25	364.8	36.6	30.51	Current study
218	220	120	5	1200	330.1	60.9	364.8	36.6	16.11	Current study
219	200	140	5	1200	330.1	60.9	364.8	36.6	17.89	Current study
220	160	160	5	1200	330.1	60.9	364.8	36.6	21.51	Current study
221	120	200	5	1200	330.1	60.9	364.8	36.6	26.51	Current study
222	107	214	5	1200	330.1	60.9	364.8	36.6	29.62	Current study
223	220	120	5	1200	330.1	51.25	364.8	36.6	18.25	Current study
224	200	140	5	1200	330.1	51.25	364.8	36.6	20.54	Current study
225	160	160	5	1200	330.1	51.25	364.8	36.6	24.51	Current study
226	120	200	5	1200	330.1	51.25	364.8	36.6	30.59	Current study
227	107	214	5	1200	330.1	51.25	364.8	36.6	32.56	Current study
228	99.5	99.5	1.82	1100	345	77.5	200	41.37	14.03	M F Hassein et al
229	99.5	99.5	1.82	1100	345	61.2	200	36.76	14.21	M F Hassein et al
230	101.7	101.7	1.85	1100	345	55.4	200	34.98	13.93	M F Hassein et al
231	101.7	101.7	1.85	1400	345	77.5	200	41.37	12.85	M F Hassein et al
232	99.5	99.5	1.82	1400	345	61.2	200	36.76	13.57	M F Hassein et al
233	99.5	99.5	1.82	1400	345	55.4	200	34.98	13.07	M F Hassein et al
234	120	200	5	1100	345	40	200	29.7	67.931	M F Hassein et al
235	107	214	5	1100	345	40	200	29.7	71.473	M F Hassein et al
236	200	120	5	1100	345	60	200	36.4	44.8	M F Hassein et al
237	178	142	5	1100	345	60	200	36.4	52.56	M F Hassein et al
238	160	160	5	1100	345	60	200	36.4	58.541	M F Hassein et al
239	120	200	5	1100	345	60	200	36.4	71.066	M F Hassein et al
240	100	200	3	1500	281	30	200	38.55	13.69	Farid et al
241	100	200	3	1500	260	30	200	38.55	13.4	Farid et al
242	100	200	3	1500	267	30	200	38.55	13.61	Farid et al
243	100	200	3	1500	270	30	200	38.55	12.79	Farid et al
244	100	200	3	1500	287	30	200	38.55	30.38	Farid et al
245	100	200	4	1500	281	50	200	38.55	30.21	Farid et al
246	100	200	4	1500	260	50	200	38.55	30.05	Farid et al
247	100	200	4	1500	267	50	200	38.55	29.19	Farid et al
248	100	200	4	1500	270	50	200	38.55	40.96	Farid et al
249	100	200	4	1500	287	50	200	38.55	39.79	Farid et al